Asymmetric Passive Dynamic Walker Used to Examine Gait Rehabilitation Methods

by

John Sushko

A thesis submitted in partial fulfillment
of the requirements for the degree of
Master of Science
Department of Mechanical Engineering
College of Engineering
University of South Florida

Major Professor: Kyle B. Reed, Ph.D.
Rajiv Dubey, Ph.D.
Jose Porteiro, Ph.D.

Date of Approval:
October 21, 2011

Keywords: model, simulation, prosthesis, PDW, transfemoral

Copyright © 2011, John Sushko

Dedication

This thesis is dedicated to my mother for her never ending support.

Acknowledgments

To my advisor Dr. Kyle B. Reed for his knowledge in programming and passive dynamics. To Craig Honeycutt for his help on this project. To Ismet Handzic for his help and encouragement. To my girlfriend Brittany Wingo for her support and understanding of all the long nights in the lab.

Table of Contents

List of Tables iii

List of Figures iv

Abstract vii

Chapter 1: Introduction to Research 1

Chapter 2: Background 4
- 2.1 Passive Dynamic Walker Models 4
- 2.2 Passive Dynamic Walkers 5
- 2.3 The Gait Dynamics of a Passive Dynamic Walker Model 8
- 2.4 Application For Rehabilitation 12

Chapter 3: Nine Mass Kneed Walker Model 14
- 3.1 Three-Link and Two-Link Dynamics 16
  - 3.1.1 The Three-Link Phase Dynamics 18
  - 3.1.2 The Two-Link Phase Dynamics 20
- 3.2 Collision Events 21
  - 3.2.1 Knee Strike 21
  - 3.2.2 Heel Strike 24
- 3.3 Nine Mass Model Results 25
  - 3.3.1 Creating a Large Asymmetry by Changing the Moment of Inertia While Keeping the Center of Mass Constant 26
  - 3.3.2 Correcting the Large Asymmetries that Arose 31
  - 3.3.3 Trends of Changing Moment of Inertia on a Passive Dynamic Walker Model 32

Chapter 4: Model Uses 40
- 4.1 Correcting a Longer Leg's Asymmetry by Adding Mass 40
- 4.2 Anthropomorphic Model 48
- 4.3 Prosthetic Model 50
  - 4.3.1 Prosthetic Model Results 51
- 4.4 Physical Walker 53

Chapter 5: Conclusions and Future Work 59
5.1 Conclusions 59
5.2 Future Work 60
5.2.1 Joint Torques 61
5.2.2 Spasticity 61
5.2.3 Human Validation 62

List of References 63

Appendices 66
Appendix A: Five Mass Model Derivation 67

List of Tables

Table 4.1 Anthropomorphic Model Mass 50

Table 4.2 Anthropomorphic Model Mass Locations 50

Table 4.3 Prosthesis Model Mass Results 53

Table 4.4 Prosthesis Model Knee Location Results 53

List of Figures

Figure 2.1 The rimless wheel 5

Figure 2.2 This shows evolution of the walker models 6

Figure 2.3 Some previous work on passive dynamic walkers 7

Figure 2.4 The symmetric step pattern 10

Figure 2.5 The single step pattern 10

Figure 2.6 The double step pattern 11

Figure 2.7 The quadruple step pattern 11

Figure 2.8 The gait enhancing mobile shoe (GEMS) 13

Figure 3.1 The nine mass model 15

Figure 3.2 The nine mass three link model 17

Figure 3.3 The nine mass two link model 17

Figure 3.4 The masses on the right leg shank are separated by 0.24m 28

Figure 3.5 The masses on the right leg thigh separated by 0.25m 29

Figure 3.6 The masses on both the shank and thigh right leg are separated by 0.07m and 0.26m 30

Figure 3.7 The symmetric solution when the shank masses on the right leg are separated by 0.24m 33

Figure 3.8 The symmetric solution when the thigh masses on the right leg are separated by 0.25m 34

Figure 3.9 The symmetric solution when the thigh masses on both the shank and thigh right leg are separated by 0.07m and 0.26m 35

Figure 3.10 The step length changing with different parameters when b1R = 0.24m 37

Figure 3.11 The step length changing with different parameters when b2R = 0.25m 38

Figure 3.12 The step length changing with different parameters when b1R = 0.07m and b2R = 0.26m 39

Figure 4.1 The plot of mt2L versus step length 41

Figure 4.2 This plot shows the gait dynamics when the right leg is 1.02m long 43

Figure 4.3 The symmetric solution when the right leg is 1.02m 44

Figure 4.4 The configuration with the largest asymmetry when the right leg is 1.02m 44

Figure 4.5 These plots show the gait dynamics when the right leg is 1.05m long 46

Figure 4.6 The symmetric solution when the right leg is 1.05m 47

Figure 4.7 The configuration with the largest asymmetry when the right leg is 1.05m 47

Figure 4.8 The anthropomorphic model 49

Figure 4.9 The prosthesis model 52

Figure 4.10 The prosthesis symmetric gait pattern when the mass is heavier than the intact leg 54

Figure 4.11 The prosthesis symmetric gait pattern when the mass is lighter than the intact leg 55

Figure 4.12 The prosthesis asymmetric gait pattern when the mass is lighter than the intact leg 56

Figure 4.13 The picture of the physical walker 57

Figure 4.14 The Solid Works drawing the physical walker 58

Abstract

Testing gait rehabilitation devices on humans can be a difficult task, due to the effects of the neurological controls of the human body. This thesis advances the use of a passive dynamic walker (PDW) tuned to have asymmetric gait patterns similar to those with physical impairments to test rehabilitation devices. A passive dynamic walker is a multi-pendulum system that has a stable gait pattern when walking down a slope without any energy inputs except the forces due to gravity. A PDW model is better suited for testing rehabilitation devices because it has been shown to resemble human gait and separates the human neurological controls from the purely dynamic aspects of walking. This research uses different asymmetric gait patterns based on an asymmetric PDW to aid in the design of current and future rehabilitation methods. There are four major parts to this research: (1) the derivation of the current nine mass PDW model, (2) the effects of changing the moment of inertia and center of mass on each leg, (3) the effects of having a leg that is longer than the other and adding masses on the opposite leg to generate a symmetric gait, and (4) the design of a theoretical prosthesis that will break the assumption that the knee on the prosthetic leg should be in the same location as the intact leg. The result of changing the moment of inertia and center of mass on each leg in the nine mass model showed that it is an improvement over the previously used five mass model. This is because the five mass model forces the center of mass to change with the moment of inertia, while the nine mass model allows these to be changed independently of each other. A theoretical prosthesis has been developed in this research that is is significantly lighter

while maintaining a symmetric gait. This was accomplished by moving the knee of the prosthetic limb below the location of the intact knee.

Chapter 1: Introduction to Research

This thesis shows the use of a passive dynamic walker (PDW) for testing rehabilitation methods and devices. A PDW is a multi-link pendulum system that exhibits a steady and stable gait when walking down a slope without any energy inputs except the forces due to gravity. This research uses PDW models because they have shown their ability to recreate a gait that is repeatable and is dynamically similar to humans [15]. The dynamics of a PDW model can be modified to produce asymmetric gait patterns that are similar to individuals with impairments. These asymmetries will be used to examine gait rehabilitation methods. A PDW is important for this purpose because it separates the mechanical aspects of walking from the neurological controls of a human. The ability to separate the neurological controls from walking is what will aid in the design and testing of rehabilitation devices. Testing gait rehabilitation devices on humans is problematic due to the cognitive influences that emerge while walking.

A large part of this research is the derivation of the nine mass PDW model and how it is an improvement over previous models. To validate this model, I explored the effects of changing the center of mass and moment of inertia of each leg. This validation focuses on the rotational inertia and center of mass of each link and relates it to the symmetry of the walker model by changing the locations of the masses on the PDW model. I also performed tests on the nine mass model to analyze different rehabilitation methods. These tests were designed to reduce the asymmetries arising from common impairments. The first test looked at correcting the asymmetry that arises when an individual has one leg that is longer than the other. This asymmetry was reduced by adding two masses on the

shorter leg. The second test was to reduce the asymmetry that transfemoral amputees experience while wearing their prostheses. This is achieved by moving the prosthetic knee location below the intact knee location and reducing the prosthetic mass.

The application of passive dynamic walkers being used for gait rehabilitation is a generally novel idea. Until now, there has not been research that links PDWs with human gait correction. The only research that has been conducted that uses non-human models for gait rehabilitation was done by Otoda. Otoda used a learning algorithm on a humanoid robot walking on a split-belt treadmill [16]. A split-belt treadmill has two belts that can move independently of each other at different speeds. It has been shown that walking on a split-belt treadmill can be used to correct gait impairments (explained in more detail later in this thesis) [18]. Otoda found that the robot was able to adapt its gait to the motion of the treadmill by changing parameters on its body [16]. One of the problems with humanoid robots is that they are very complex so the number of variables greatly increases. Also, the study of non-human gait asymmetries is rather new. Gregg et al. focused on biped asymmetries arising from changing physiological or environmental conditions on the biped [8]. Examples of some of these changing conditions are the ramp angle and the initial angular positions and velocities. My research of using a passive dynamic walker to study gait dynamics for rehabilitation methods is original.

Another important reason for this research is all prior research used the five mass model (explained in detail later in this thesis). I have extended this to a nine mass model by adding an extra mass on each individual link of the walker, four in total. My hypothesis is that adding the four more masses will better describe the mass distribution of physical legs. This is because I can tune the moment of inertia to be similar to that of a human. I think that having these extra masses will better aid in the tuning of physical passive dynamic walkers. The five mass model forces the moment of inertia to change when the center of mass is changed, which is not ideal for tuning. With the nine mass model I can

change the moment of inertia independent of the center of mass. Tuning a PDW with the moment of inertia of the leg links is of greater importance than the location of the center of mass. This model is currently being used for designing and tuning the physical PDW in [10]. The ability to change the moment of inertia while keeping the center of mass constant expedited the tuning phase of the walker. This is because it can be used for cause and effect scenarios. For example, the model can be used to test new design configurations on the walker before actually being applied to the physical walker. The physical PDW is detailed in [10] and discussed some later in this thesis.

Chapter 2: Background

This thesis presents the derivation and application of a mathematical model of a two dimensional planar walker. The model is based upon the principles of passive dynamic walking and will be implemented to test gait rehabilitation techniques. This chapter will discuss the history of passive dynamics, the previous walker models, gait dynamics of the models, and how it can be used for rehabilitation.

2.1 Passive Dynamic Walker Models

"A passive dynamic walker (PDW) is a device that exhibits a steady and stable gait down a slope without any energy inputs except the forces due to gravity" [11]. The dynamics of a passive dynamic walker approximate the gait dynamics of a human accurately [15]. An important part of the study of passive dynamic walkers is the mathematical models that describe the walker's dynamics. The first theoretical model that describes gait dynamics and locomotion was created by Margaria in 1976. Margaria stated that human gait dynamics are similar to that of a rimless wheel rolling down a hill. The rimless wheel shown in Figure 2.1 has massless spokes and a single point mass at the center. The rimless wheel eventually settles into an equilibrium [13]. McGeer used the rimless wheel dynamics to derive equations that describe the first PDW model. McGeer noticed that the equilibrium that a PDW settles into is similar to the equilibrium that the rimless wheel exhibits [15]. Out of McGeer's research came the compass gait model. This model relates walking to passive dynamics in the simplest form [6]. The compass gait model is a double pendulum

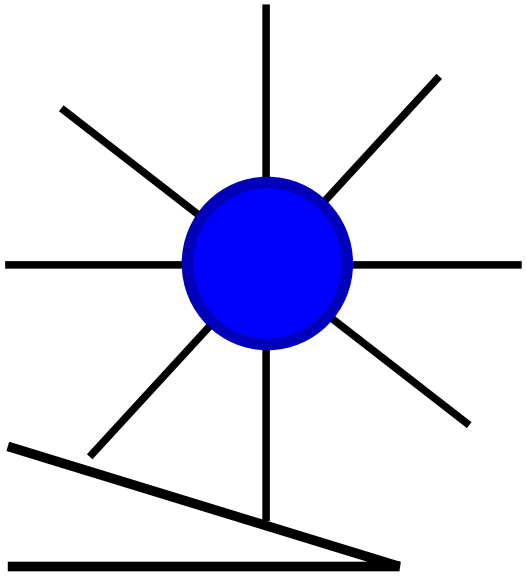

Figure 2.1: The rimless wheel

system with two leg masses and a hip mass, which follows human like gait patterns [7]. The compass gait model is shown in Figure 2.2a. In 2005, Chen advanced the compass gait model by adding knees and two more masses, as shown in Figure 2.2b. Chen created a full mathematical model for this system similar to the equations derived for the compass gait [1]. I then extended Chen's research by differentiating between the left and right leg. This is the five mass model which lets us change specific parameters on each leg to find asymmetric gait patterns . The five mass model can be seen in Figure 2.2c. Figure 2.2c shows that the right leg (green) is different from the left leg (blue). Figure 2.2 shows a flow chart that depicts the evolution of the walker models starting with the compass gait [7], then Chen's kneed model [1], the five mass model [11], and finally the nine mass model.

2.2 Passive Dynamic Walkers

Some of the walkers that have been previously designed and made can be seen in Figure 2.3. Starting on the left is McGeer's walker, that he designed in the 1980's [15]. McGeer's

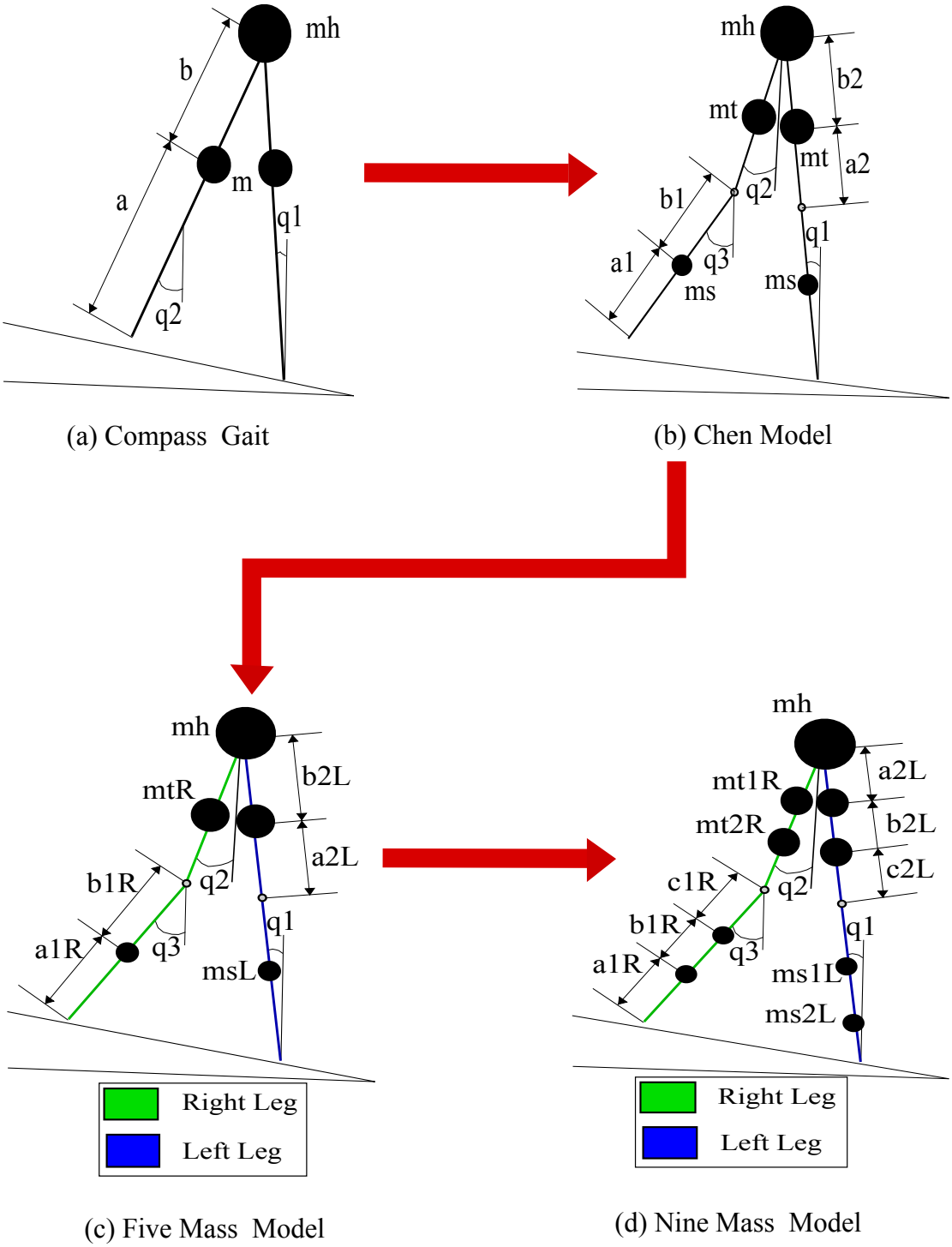

(a) Compass Gait

(b) Chen Model

(c) Five Mass Model

(d) Nine Mass Model

Figure 2.2: This shows evolution of the walker models. Starting with the compass gait [7], Chen's kneed model [1], the five mass model [11], and the nine mass model.

Figure 2.3: Some previous work on passive dynamic walkers. Left to Right: McGeer's first walker [15]; The Cornell biped with arms [3]; The Cornell Ranger [12]; The TU Delft MIKE Robot [21].

first walker was very interesting because it did not have knees but instead used motors to lift up the feet to clear the ground on each step. McGeer mentions in his paper that to have the feet clear the ground one of the following techniques has to be employed: his ankle actuation, a walker that waddles from left to right, or knees [15]. Second from the left is the Cornell biped with arms [3]. This biped best describes the human gait. Due to its swinging arms it better represents the human trunk. Third from the left is the Cornell ranger which holds the record for longest distance traveled by a PDW of 40.5 miles. The Ranger has actuators on the ankles to add in the energy at heel-strike [12]. The walker farthest on the right is the Tu Delft MIKE robot. It is an autonomous walking robot based on a PDW. The MIKE robot has minimal amounts of actuation at the knees and foot to add energy into the system. The actuators are pneumatic and have to be very light and efficient to add the needed amount of energy but light enough to not affect the dynamics. The actuators essentially act as muscles for the robot [21].

2.3 The Gait Dynamics of a Passive Dynamic Walker Model

In preliminary research for this thesis, one dimensional tests were used to evaluate the effects of changing the magnitude of the link masses, the location of the the link masses and the position of the knee [11]. This research evaluated the previously mentioned five mass model. The five mass model can be seen in Figure 2.2c. Parameters were changed on the right leg of the five mass model to alter its gait pattern from symmetry. Specific parameters were changed to create different model configurations. Asymmetries arose from some of these configurations. For a model configuration to be a successful configuration, it had to walk for fifty steps. The asymmetries are defined by having step lengths of the left and right leg that are not equal. Step length is the distance between the legs when the swing leg makes contact with the ground. After changing the parameters, four different gait patterns emerged:

1. *Symmetric step pattern*: This pattern is normal symmetric walking where both step lengths quickly converge to one value. This gait pattern best represents human gait, as seen in Figure 2.4.

2. *The leg specific single step pattern*: For this pattern, each leg has its own specific step length. This is the most stable step pattern besides the symmetric pattern. This pattern best represents an asymmetric gait pattern of a human who has suffered a stroke or other impairments. An example of the single step pattern can be seen in Figure 2.5.

3. *Leg specific double step pattern*: Whereas in the single step pattern each leg has its own step length, in the double step pattern each leg has two unique step lengths. Looking at Figure 2.6, the right leg always has a longer step length than the left leg. Step 2 corresponds to the first right leg step in the cycle. This occurs when the right leg is swinging. Figure 2.6 also shows that step 2 is always the longest.

4. *Leg specific quadruple step pattern*: This is the most interesting gait pattern produced in [11]. Similar to the double step, step 2 will always have the longest step length. There are now four specific step lengths for each leg. The gait pattern can be seen in Figure 2.7.

These gait patterns were a study of interesting dynamics and gives a basis on the dynamics of walking. The single step pattern will be useful for modeling gait patterns of humans with impairments, but the research done in [11] does not take any major steps toward rehabilitation. That being said, it did give insight into the effects of changing different design parameters. The research done in [11] produced useful descriptions of the symmetry on a PDW model configuration. The top of Figures 2.4 through 2.7 show two different plots. The plot on the left is the step length plot, which compares the step length versus the step number, and is the main measuring tool for symmetry. On the right is the limit cycle trajectory, which depicts the motion in each phase of of the PDW's gait. The limit cycle plot shows the angle in radians versus angular velocity in radians per second. Figure 2.5 describes the limit cycle plot and what each color line depicts. This plot follows the right leg in every part of its dynamics. This plot directly relates to the kinetic and potential energy of the right leg. Red and green are the three-link and two-link phases while the right leg is swinging. There is a jump between the red and green lines that shows the energy change after knee strike. After the green line, there is another jump that separates the blue line, which is the energy change from heel strike. The blue and black lines are the three-link and two link phases when the right leg is the stance leg. The jump between the back and blue lines is the energy changed due to knee strike of the left leg. The energy change between the black and red line is the heel strike event for the left leg. The cycle starts back with the red line where the right leg is swinging in three-link phase. These dynamics will be explained in better detail later in this thesis when the current PDW model is described.

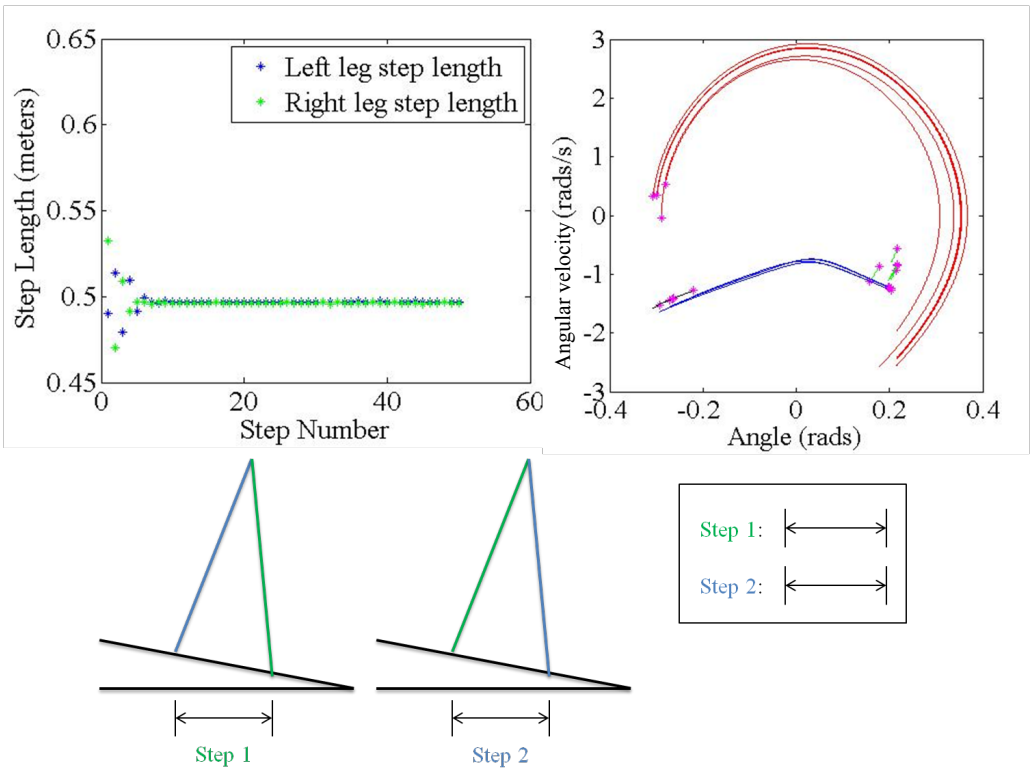

Figure 2.4: The symmetric step pattern.

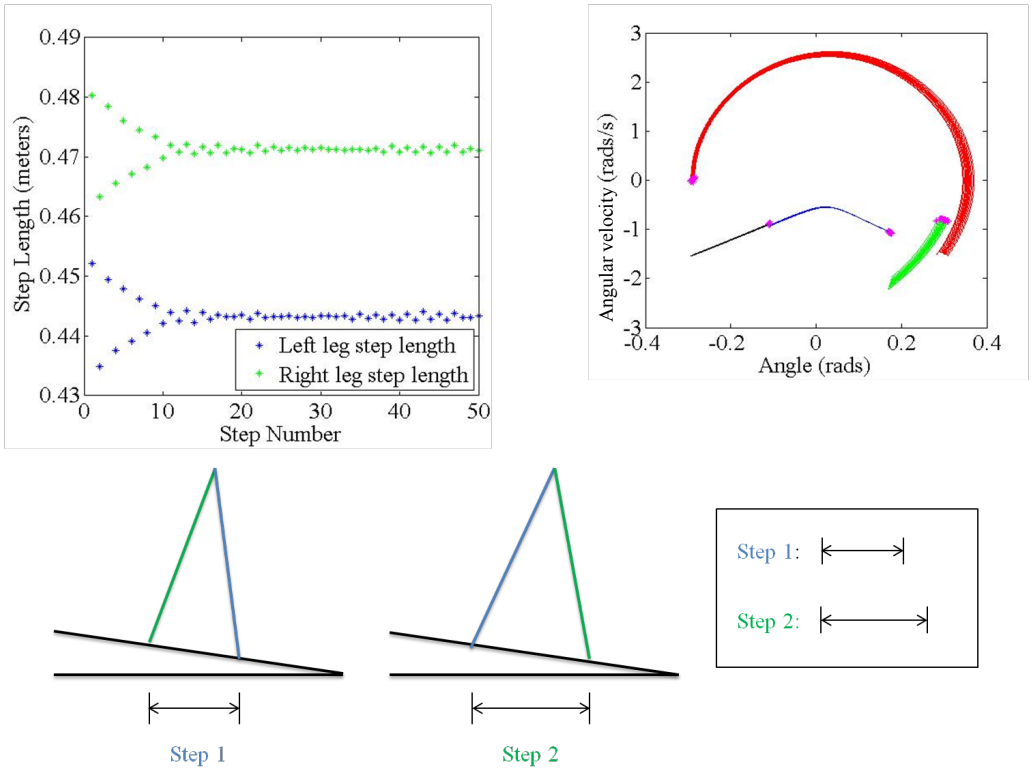

Figure 2.5: The single step pattern.

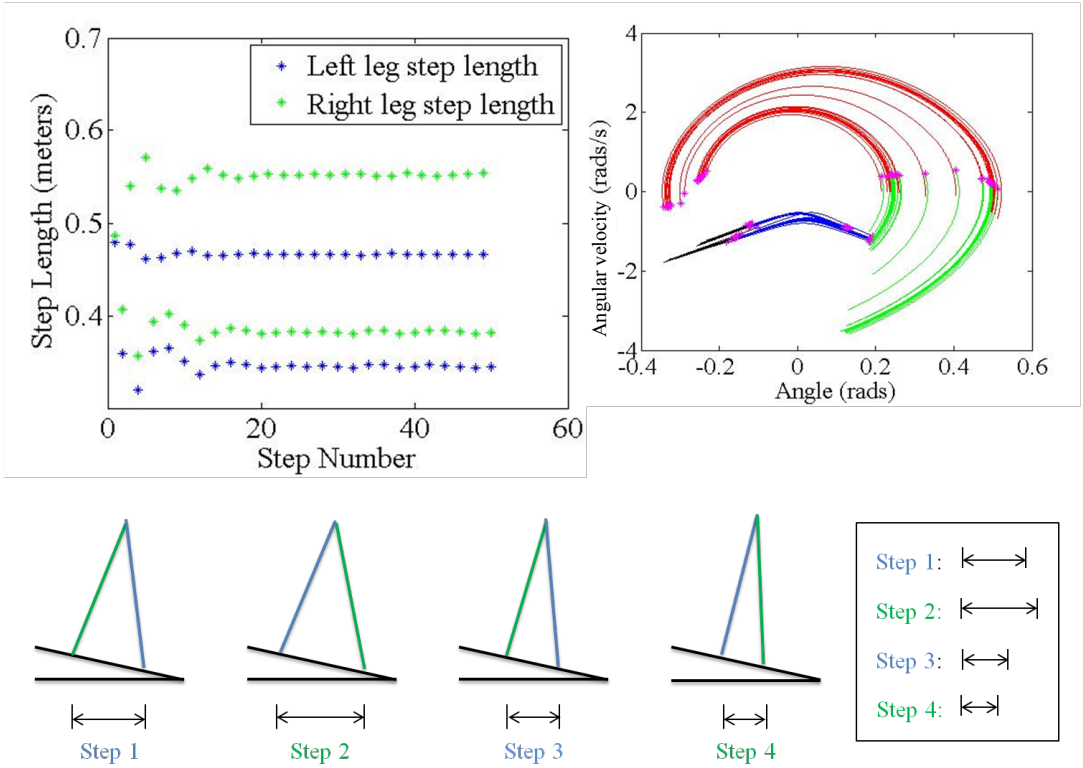

Figure 2.6: The double step pattern.

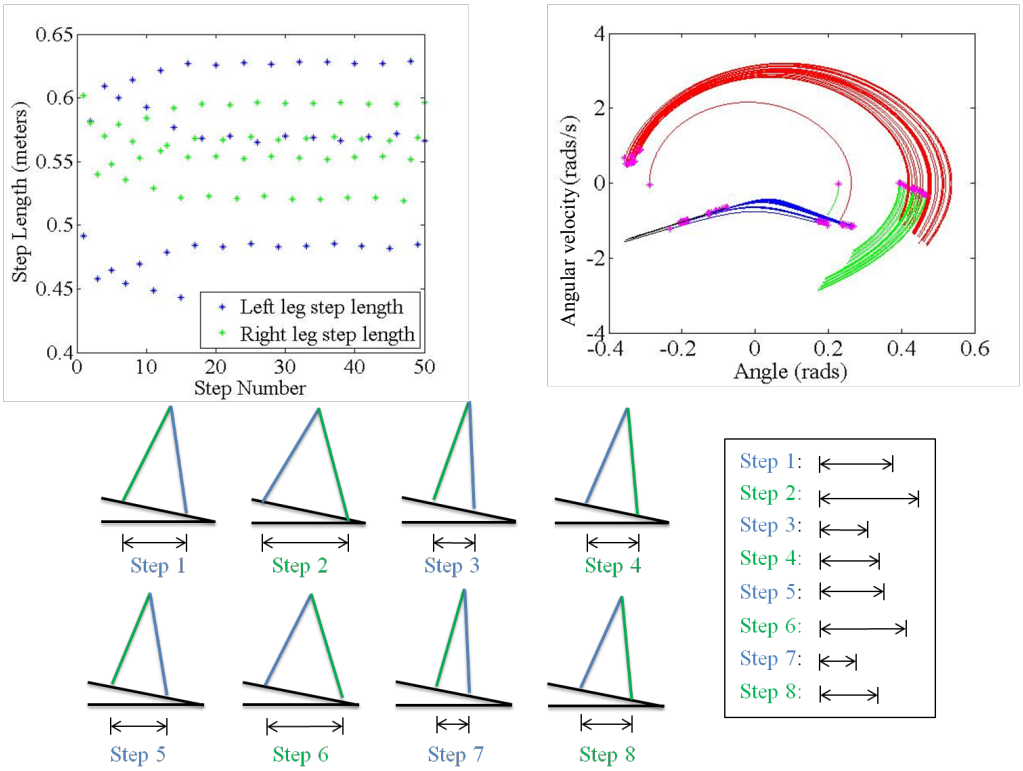

Figure 2.7: The quadruple step pattern.

2.4 Application For Rehabilitation

As stated above, currently the only research being done that uses non-human models for gait rehabilitation uses humanoid robots. Humanoid robots were not chosen for this research because their gait does not model the gait of a human very accurately. The reason for this is because humanoid robots walk in a quasi-static manor, meaning that the way they achieve equilibrium is statically. So a humanoid robot can stop at any point in its gait. The most notable humanoid robot is the Honda AISMO, which demonstrates very clearly a non-human gait. Humans on the other hand walk in a dynamic equilibrium. There are points in a human's gait pattern where they cannot stop because they will fall. A human's gait can be described as perpetual free fall. A PDW has as similar gait pattern to a human because it can also only achieve equilibrium dynamically. This makes PDWs ideal to test rehabilitation methods and devices. PDWs allow the ability to examine different asymmetric gait patterns without the cognitive influence of human neurological controls. This is important when studying individuals with neurological disorders like someone who suffered a stroke and will aid in the design of rehabilitation devices.

One of these devices I would like to examine is the Gait Enhancing Mobile Shoe (GEMS) [4][9]. The GEMS is a rehabilitation shoe that focuses on correcting human asymmetric gaits. The GEMS is shown in Figure 2.8. Studies have shown that the use of split-belt treadmill training can correct asymmetric gaits. A split-belt treadmill is a treadmill that has two treads that can each move at different speeds allowing for control of each of the participant's legs independently. This ability for control is what allows for the gait correction because it forces the lagging leg to walk at a faster rate, which exaggerates the asymmetry and generates an after-effect that is the correct gait. The effects of split-belt treadmill rehabilitation diminish quickly when the participants start walking on solid ground [18][2]. It is not clearly known why these effects diminish so quickly. One major hypothesis is that the perception while walking on the treadmill differs greatly from walk-

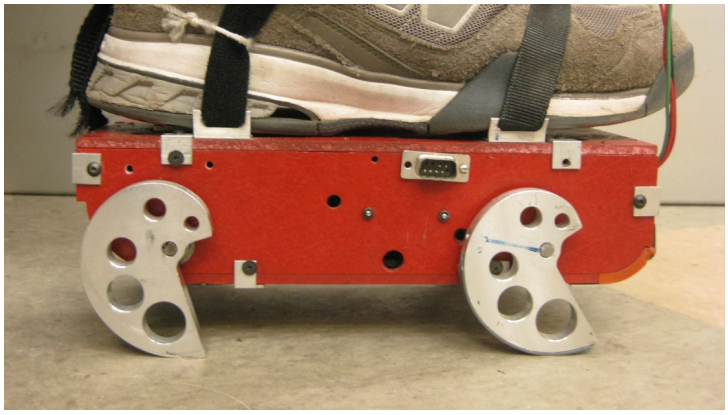

Figure 2.8: The gait enhancing mobile shoe (GEMS). [9]

ing on solid ground. The GEM shoe replicates the backwards motion that the split-belt treadmill produces, but allows the participant to walk on solid ground [9]. If the GEM shoe could be modeled mathematically, it could be imposed on one of the feet in the nine mass model to correct a theoretical asymmetric gait.

The nine mass model could be applied to transfemoral prosthesis design. Individuals who wear a prostheses typically have an asymmetry where their prosthetic leg has a step length that is longer than their intact leg. Because of this asymmetry and the weight of the prosthesis, individuals with a prosthetic limb use more energy when walking than individuals with both legs intact [14]. Mattes et al. discuss that a symmetric gait pattern and weight reduction reduce the energy used while walking [14]. My model is used in this thesis to find a symmetric gait pattern for a prosthesis that is also significantly lighter.

Chapter 3: Nine Mass Kneed Walker Model

A kneed passive dynamic walker can be modeled as a multi-pendulum system that is unactuated. The first iteration of the model was done by Chen [1], who took the compass gait model and added knees, thus making it a more human like model. I took this further in my model by differentiating between each leg. The two legs are the stance leg (st), which is the leg that is in contact with the ground, and the swing leg (sw), which is the leg swinging freely. Using swing and stance makes the equations more general. In practice the equations have to be written twice in terms of right and left leg changing from stance to swing. For example, one set of equations describe when the left leg is the stance leg and the other set would describe when the right leg is the stance leg. This differentiation is used to develop asymmetries by changing parameters on each leg. I call this model the five mass system and it is shown in Figure 2.2c. To better develop asymmetries, I added another mass on each link making a nine mass system. The nine mass model is seen in Figure 2.2d and in Figure 3.2. With this model, I can more accurately describe the leg mass distribution. The nine masses are the hip mass (mh), the upper shank mass on the stance leg ($ms2_{st}$), the lower shank mass on the stance leg ($ms1_{st}$), the upper thigh mass on the stance leg ($mt1_{st}$), the lower thigh mass on the stance leg ($mt2_{st}$), the upper shank mass on the swing leg ($ms2_{sw}$), the lower shank mass on the swing leg ($ms1_{sw}$), the upper thigh mass on the swing leg ($mt1_{sw}$), and the lower thigh mass on the swing leg ($mt2_{sw}$). The bottom rods are the shank links and the top rods are the thigh links. The shank length is $ls = a1 + b1 + c1$ and the thigh length is $lt = a2 + b2 + c2$, both in terms of st and sw. The total length is $L = ls + lt$, also in terms if st and sw.

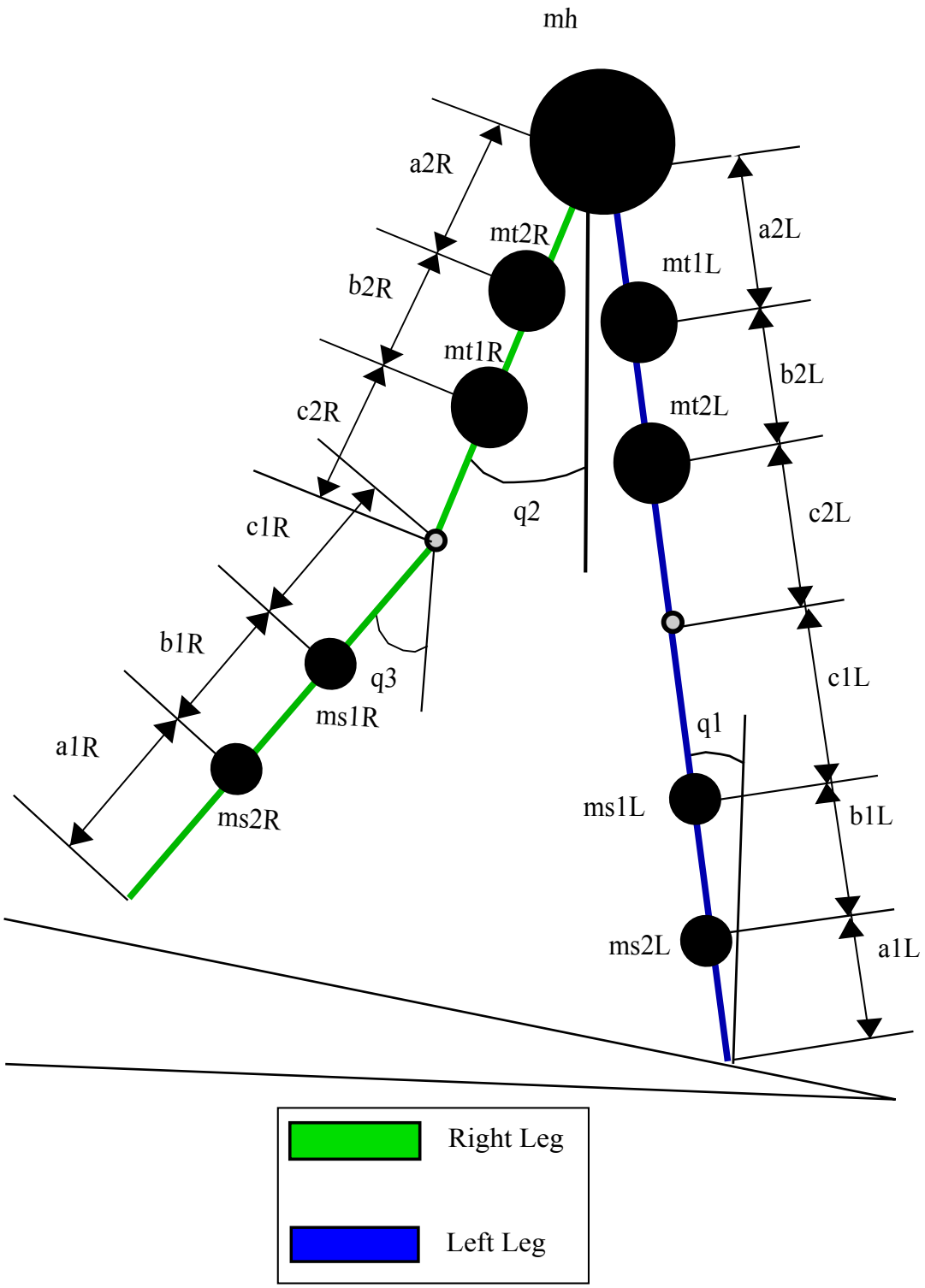

Figure 3.1: The nine mass model.

The nine mass system better approximates human legs and physical passive dynamic walker legs because I can better approximate the mass distribution. Also as stated previously, I am able to fine tune the moment of inertia to whatever model I am trying to examine. The nine mass model is an improvement over the five mass system because of the amount of adjustably and versatility it provides. The five mass model has also been derived, in Appendix A.

The walker goes through two distinct stages in its dynamics: a two-link phase and a three-link phase. The three-link phase is the starting phase for the walker. The three-link phase is shown in Figure 3.2. From these figures it can be seen that L_{st} is connected to the hip, which is in turn connected to lt_{sw}. The knee is what joins ls_{sw} to lt_{sw}. The walker stays in the three-link phase until the knee strike event. After knee strike occurs, the knee is locked and the system is a double pendulum. This double pendulum system is the two-link phase shown in the nine mass model of Figure 3.3. The walker is in two-link phase until the heel strike event. Heel strike finishes the cycle of the walker and three-link starts again. The two-link phase has two links L_{st} and L_{sw}, which are connected together by the hip.

3.1 Three-Link and Two-Link Dynamics

The walker's dynamics can be derived using the Lagrangian formulation for a multi-pendulum system shown in (3.1). The three matrices in this equation H, B, and G are the inertia, velocity, and gravity matrices respectively. The components of these matrices will be described in the following equations.

$$H(q)\ddot{q} + B(q, \dot{q})\dot{q} + G(q) = 0 \tag{3.1}$$

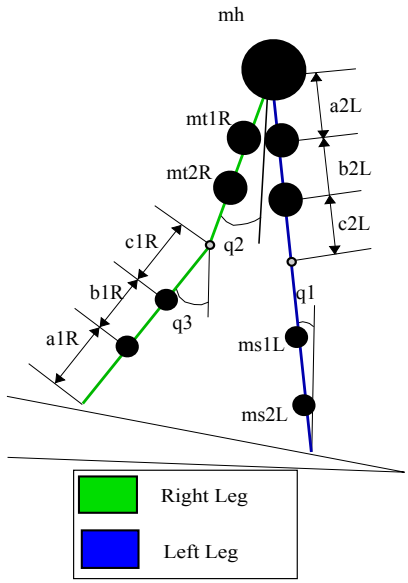

Figure 3.2: The nine mass three link model.

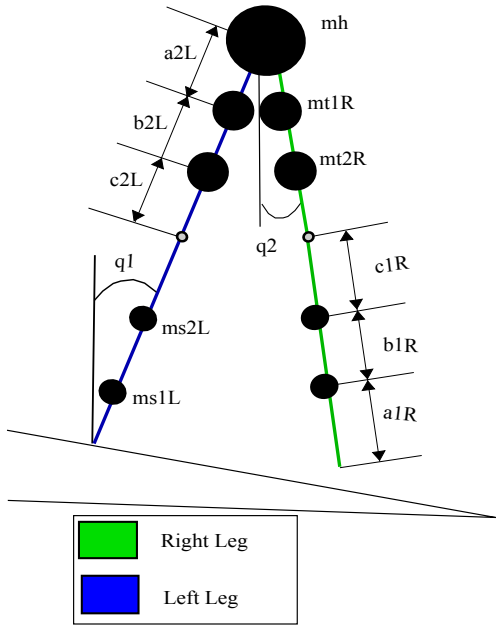

Figure 3.3: The nine mass two link model.

3.1.1 The Three-Link Phase Dynamics

The three-link dynamics were derived using the Lagrangian formulation for a pendulum system with multiple links. The three-link inertia matrix for a nine mass system is derived in the following equations:

$$\begin{aligned} H11 = {} & ms1_{st}a1_{st}^2 + ms2_{st}(a1_{st} + b1_{st})^2 + \\ & mt2_{st}(ls_{st} + c2_{st})^2 + mt1_{st}(ls_{st} + c2_{st} + b2_{st})^2 + \\ & (mh + ms1_{sw} + ms2_{sw} + mt1_{sw} + mt2_{sw})L_{st}^2 \end{aligned} \tag{3.2}$$

$$\begin{aligned} H12 = {} & -[mt1_{sw}a2_{sw} + mt2_{sw}(a2_{sw} + b2_{sw}) + \\ & ms1_{sw}lt_{sw} + ms2_{sw}lt_{sw}]L_{st}\cos(q_2 - q_1) \end{aligned} \tag{3.3}$$

$$H13 = -[ms2_{sw}c1_{sw} + ms1_{sw}(c1_{sw} + b1_{sw})]L_{st}\cos(q_3 - q_1) \tag{3.4}$$

$$H21 = H12 \tag{3.5}$$

$$H22 = mt1_{sw}a2_{sw}^2 + mt2_{sw}(a2_{sw} + b2_{sw})^2 + ms1_{sw}lt_{sw}^2 + ms2_{sw}lt_{sw}^2 \tag{3.6}$$

$$H23 = [ms2_{sw}c1_{sw} + ms1_{sw}(c1_{sw} + b1_{sw})]lt_{sw}\cos(q_3 - q_2) \tag{3.7}$$

$$H31 = H13 \tag{3.8}$$

$$H32 = H23 \tag{3.9}$$

$$H33 = ms2_{sw}c1_{sw}^2 + ms1_{sw}(c1_{sw} + b1_{sw})^2 \tag{3.10}$$

$$H = \begin{bmatrix} H11 & H12 & H13 \\ H21 & H22 & H23 \\ H31 & H32 & H33 \end{bmatrix} \tag{3.11}$$

The three-link velocity matrix for the 9 mass system is derived in the following equations:

$$\begin{aligned} h122 = -[mt1_{sw}a2_{sw} + mt2_{sw}a2_{sw} + b2_{sw}) + \\ ms1_{sw}lt_{sw} + ms2_{sw}lt_{sw}]L_{st}\sin(q_2 - q_1) \end{aligned} \tag{3.12}$$

$$h133 = -[ms2_{sw}c1_{sw} + ms1_{sw}(c1_{sw} + b1_{sw})]L_{st}\sin(q_3 - q_1) \tag{3.13}$$

$$h211 = -h122 \tag{3.14}$$

$$h233 = [ms2_{sw}c1_{sw} + ms1_{sw}(c1_{sw} + b1_{sw})]lt_{sw}\sin(q_3 - q_2) \tag{3.15}$$

$$h311 = -h133 \tag{3.16}$$

$$h322 = -h233 \tag{3.17}$$

$$B = \begin{bmatrix} 0 & h122\dot{q}_2 & h133\dot{q}_3 \\ h211\dot{q}_2 & 0 & h233\dot{q}_3 \\ h311\dot{q}_1 & h322\dot{q}_2 & 0 \end{bmatrix} \tag{3.18}$$

The gravity matrix for the 9 mass system in the three-link phase is derived in the following equations:

$$\begin{aligned} g_1 = -[ms1_{st}a1_{st} + ms2_{st}(a1_{st} + b1_{st}) + \\ mt2_{st}(ls_{st} + c2_{st}) + mt1_{st}(ls_{st} + a2_{st} + b2_{st}) + \\ (mh + ms1_{sw} + ms2_{sw} + mt1_{sw} + mt2_{sw})L_{sw}]\sin(q_1)g \end{aligned} \tag{3.19}$$

$$\begin{aligned} g_2 = [mt1_{sw}a2_{sw} + mt2_{sw}(a2_{sw} + b2_{sw}) + \\ ms1_{sw}lt_{sw} + ms1_{sw}lt_{sw}]\sin(q_2)g \end{aligned} \tag{3.20}$$

$$g_3 = [ms2_{sw}c1_{sw} + ms1_{sw}(b1_{sw} + c1_{sw})]\sin(q_3)g \tag{3.21}$$

$$G = [g_1 \;\; g_2 \;\; g_3]^T \tag{3.22}$$

3.1.2 The Two-Link Phase Dynamics

The two-link phase equations are similar to the three-link except less complicated. Due to the fact that the knee is locked for the two-link phase the amount of terms are reduced. The two-link inertia matrix is derived in the following equations:

$$\begin{aligned} H11 = {} & ms1_{st}a1_{st}^2 + ms2_{st}(a1_{st} + b1_{st})^2 + \\ & mt2_{st}(ls_{st} + c2_{st})^2 + mt1_{st}(ls_{st} + c2_{st} + a2_{st})^2 + \\ & (mh + ms1_{sw} + ms2_{sw} + mt1_{sw} + mt2_{sw})L_{st}^2 \end{aligned} \tag{3.23}$$

$$\begin{aligned} H12 = {} & -[mt1_{sw}a2_{sw} + mt1_{sw}(a2_{sw} + b2_{sw}) + ms2_{sw}(lt_{sw} + c1_{sw}) + \\ & ms1_{sw}(lt_{sw} + b1_{sw} + c1_{sw})]L_{st}\cos(q_2 - q_1) \end{aligned} \tag{3.24}$$

$$H21 = H12 \tag{3.25}$$

$$\begin{aligned} H22 = {} & mt1_{sw}a2_{sw}^2 + mt2_{sw}(a2_{sw} + b2_{sw})^2 + \\ & ms2_{sw}(lt_{sw} + c1_{sw})^2 + ms1_{sw}(lt_{sw} + c1_{sw} + b1_{sw}) \end{aligned} \tag{3.26}$$

$$H = \begin{bmatrix} H11 & H12 \\ H21 & H22 \end{bmatrix} \tag{3.27}$$

The Lagrangian velocity matrix for the two-link phase:

$$\begin{aligned} h = {} & -[mt1_{sw}a2_{sw} + mt2_{sw}(a2_{sw} + b2_{sw}) + ms2_{sw}(lt_{sw} + c1_{sw}) + \\ & ms1_{sw}(lt_{sw} + b1_{sw} + c1_{sw})]L_{st}\sin(q_2 - q_1) \end{aligned} \tag{3.28}$$

$$B = \begin{bmatrix} 0 & h\dot{q}_2 \\ -h\dot{q}_1 & 0 \end{bmatrix} \tag{3.29}$$

$$
\begin{aligned}
g_1 = -[&ms1_{st}a1_{st} + ms2_{st}(a1_{st} + b1_{st}) + \\
&mt2_{st}(ls_{st} + c2_{st}) + mt1_{st}(ls_{st} + a2_{st} + c2_{st}) + \\
&(mh + ms1_{sw} + ms2_{sw} + mt1_{sw} + mt2_{sw})L_{sw}]\sin(q_1)g
\end{aligned} \tag{3.30}
$$

$$
\begin{aligned}
g_2 = [&mt1_{sw}a2_{sw} + mt2_{sw}(a2_{sw} + b2_{sw}) + \\
&ms2_{sw}(lt_{sw} + c1_{sw}) + ms1_{sw}(lt_{sw} + b1_{sw} + c1_{sw})]\sin(q_2)g
\end{aligned} \tag{3.31}
$$

$$
G = \begin{bmatrix} g_1 \\ g_2 \end{bmatrix} \tag{3.32}
$$

3.2 Collision Events

The collision events, as mentioned earlier, are the knee strike and heel strike. These collisions are modeled as inelastic and instantaneous. They are derived from the conservation of angular momentum about the appropriate point for the specific collision.

3.2.1 Knee Strike

The knee strike collision is the collision that changes the walker from the three-link phase to the two-link phase. The collision is considered inelastic due to the fact that the knee stays locked through the two-link phase.

The following equations take the pre-collision velocities (q^-) and apply conservation of angular momentum and output the post-collision velocities (q^+). It is to be noted that the superscript $+$ is post-collision and $-$ is pre-collision.

$$
\begin{bmatrix} \dot{q_1}^+ \\ \dot{q_2}^+ \end{bmatrix} = Q^{+-1} \begin{bmatrix} \dot{q_1}^- \\ \dot{q_2}^- \\ \dot{q_3}^- \end{bmatrix} Q^- \tag{3.33}
$$

$$\alpha = q_1 - q_2 \tag{3.34}$$

$$\beta = q_1 - q_3 \tag{3.35}$$

$$\gamma = q_2 - q_3 \tag{3.36}$$

$$\begin{aligned} Q_{11}^{+} = Q_{21}^{+} + mt2_{st}(ls_{st} + c2_{st})^2 + mt1_{st}(ls_{st} + b2_{st} + c2_{st})^2 + \\ (mh + mt1_{st} + mt2_{st} + ms1_{st} + ms2_{st})L_{st}^2 + \\ ms1_{st}a1_{st}^2 + ms2_{st}(a1_{st} + b1_{st})^2 \end{aligned} \tag{3.37}$$

$$\begin{aligned} Q_{12}^{+} = Q_{21}^{+} + ms2_{sw}(lt_{sw} + c1_{sw})^2 + ms1_{sw}(lt_{sw} + b1_{sw} + c1_{sw})^2 + \\ mt1_{sw}a2_{sw}^2 + mt2_{sw}(a2_{sw} + b2_{sw})^2 \end{aligned} \tag{3.38}$$

$$\begin{aligned} Q_{21}^{+} = -[ms2_{sw}(c1_{sw} + lt_{sw}) + ms1_{sw}(c1_{sw} + b1_{sw} + lt_{sw}) \\ mt1_{sw}a2_{sw} + mt2_{sw}(a2_{sw} + b2_{sw})]L_{st}\cos(\alpha) \end{aligned} \tag{3.39}$$

$$\begin{aligned} Q_{22}^{+} = ms2_{sw}(lt_{sw} + c1_{sw})^2 + ms1_{sw}(lt_{sw} + b1_{sw} + c1_{sw})^2 \\ mt1_{sw}a2_{sw}^2 + mt2_{sw}(a2_{sw} + b2_{sw})^2 \end{aligned} \tag{3.40}$$

$$\begin{aligned} Q_{11}^{-} = -[ms1_{sw}lt_{sw} + ms2_{sw}lt_{sw} + \\ mt1_{sw}a2_{sw}mt2_{sw}(a2_{sw} + b2_{sw})]L_{st}\cos(\alpha) \\ -[ms2_{sw}c1_{sw} + ms2_{sw}(b1_{sw} + c1_{sw})]L_{st}\cos(\beta) + \\ [ms1_{sw} + ms2_{sw} + mt1_{sw} + mt2_{sw}]L_{st}^2 + \\ ms1_{st}a1_{st}^2 + ms2_{sw}(a1_{sw} + b1_{sw})^2 + \\ mt2_{st}(ls_{st} + c2_{st}) + mt1_{st}(ls_{st} + b2_{st} + c2_{st}) \end{aligned} \tag{3.41}$$

$$
\begin{aligned}
Q_{12}^{-} = -[&ms1_{sw}lt_{sw} + ms2_{sw}lt_{sw}+ \\
&mt1_{sw}a2_{sw} + mt2_{sw}(a2_{sw} + b2_{sw})]L_{st}\cos(\alpha)+ \\
&[ms2_{sw}c1_{sw} + ms1_{sw}(b1_{sw} + c1_{sw})]lt_{sw}\cos(\gamma)+ \\
&mt1_{sw}a2_{sw}^2 + mt2_{sw}(a2_{sw} + b2_{sw})^2+ \\
&ms1_{sw}lt_{sw}^2 + ms2_{sw}lt_{sw}^2
\end{aligned} \tag{3.42}
$$

$$
\begin{aligned}
Q_{13}^{-} = -[&ms2_{sw}c1_{sw} + ms2_{sw}(b1_{sw} + c1_{sw})]L_{st}\cos(\beta)+ \\
&[ms2_{sw}c1_{sw} + ms1_{sw}(b1_{sw} + c1_{sw})]lt_{sw}\cos(\gamma)+ \\
&ms2_{sw}c1_{sw}^2 + ms1_{sw}(b1_{sw} + c1_{sw})^2
\end{aligned} \tag{3.43}
$$

$$
\begin{aligned}
Q_{21}^{-} = -[&ms1_{sw}lt_{sw} + ms2_{sw}lt_{sw}+ \\
&mt1_{sw}a2_{sw} + mt2_{sw}(a2_{sw} + b2_{sw})]L_{st}\cos(\alpha)+ \\
&-[ms2_{sw}c1_{sw} + ms2_{sw}(b1_{sw} + c1_{sw})]L_{st}\cos(\beta)
\end{aligned} \tag{3.44}
$$

$$
\begin{aligned}
Q_{22}^{-} = &[ms2_{sw}c1_{sw} + ms1_{sw}(b1_{sw} + c1_{sw})]lt_{sw}\cos(\gamma)+ \\
&mt1_{sw}a2_{sw}^2 + mt2_{sw}(a2_{sw} + b2_{sw})^2+ \\
&ms1_{sw}lt_{sw}^2 + ms2_{sw}lt_{sw}^2
\end{aligned} \tag{3.45}
$$

$$
\begin{aligned}
Q_{23}^{-} = &[ms2_{sw}c1_{sw} + ms1_{sw}(b1_{sw} + c1_{sw})]lt_{sw}\cos(\gamma)+ \\
&ms2_{sw}c1_{sw}^2 + ms1_{sw}(b1_{sw} + c1_{sw})^2
\end{aligned} \tag{3.46}
$$

$$
Q^{+} = \begin{bmatrix} Q_{11}^{+} & Q_{12}^{+} \\ Q_{12}^{+} & Q_{22}^{+} \end{bmatrix} \tag{3.47}
$$

$$
Q^{-} = \begin{bmatrix} Q_{11}^{-} & Q_{12}^{-} & Q_{13}^{-} \\ Q_{12}^{-} & Q_{22}^{-} & Q_{23}^{-} \end{bmatrix} \tag{3.48}
$$

3.2.2 Heel Strike

The heel strike event is when the walker finishes the two-link phase by the swing foot impacting with the ground. After the impact the swing foot then becomes the stance foot and the walker starts the three-link phase and rotates around the new stance foot.

$$q^+ = \begin{bmatrix} q_2^- \\ q_1^- \\ q_1^- \end{bmatrix} \tag{3.49}$$

$$\begin{bmatrix} \dot{q_1}^+ \\ \dot{q_2}^+ \\ \dot{q_3}^+ \end{bmatrix} = Q^{+-1} \begin{bmatrix} \dot{q_1}^- \\ \dot{q_2}^- \end{bmatrix} Q^- \tag{3.50}$$

$$\dot{q}_3^+ = \dot{q}_2^+ \tag{3.51}$$

$$\alpha = q_1 - q_2 \tag{3.52}$$

$$\begin{aligned} Q_{11}^+ = Q_{21}^+ + ms1_{sw}a1_{sw}^2 + ms2_{sw}(a1_{sw} + b1_{sw})^2 + \\ mt1_{sw}(c2_{sw} + b2_{sw} + ls_{sw}) + mt2_{sw}(c2_{sw} + ls_{sw})^2 + \\ (ms1_{st} + ms2_{st} + mt1_{st} + mt2_{st})L_{sw}^2 \end{aligned} \tag{3.53}$$

$$\begin{aligned} Q_{12}^+ = Q_{21}^+ + ms2_{st}(c1_{st} + lt_{st})^2 + ms1_{st}(c1_{st} + b1_{st} + lt_{st}) + \\ mt1_{st}a2_{st}^2 + mt2_{st}(a2_{st} + b2_{st})^2 \end{aligned} \tag{3.54}$$

$$\begin{aligned} Q_{21}^+ = -[ms1_{st}(c1_{st} + b1_{st} + lt_{st}) + ms2_{st}(c1_{st} + lt_{st}) + \\ mt1_{st}a2_{st} + mt2_{st}(a2_{st} + b2_{st})]L_{sw}\cos(\alpha) \end{aligned} \tag{3.55}$$

$$\begin{aligned} Q_{22}^+ = mt1_{st}a2_{st}^2 + mt2_{st}(a2_{st} + b2_{st})^2 + \\ ms2_{st}(lt_{st} + c1_{st})^2 + ms1_{st}(lt_{st} + b1_{st} + c1_{st})^2 \end{aligned} \tag{3.56}$$

$$
\begin{aligned}
Q_{11}^{-} = Q_{12}^{-} + [&mhl_{st} + 2mt2_{st}(c2 + ls_{st}) + \\
&2mt1_{st}(c2_{st} + b2_{st} + ls_{st}) + \\
&ms1_{st}a1_{st} + ms2_{st}(a1_{st} + b1_{st})]L_{st}\cos(\alpha)
\end{aligned} \tag{3.57}
$$

$$
\begin{aligned}
Q_{12}^{-} = -[&ms1_{sw}a1_{sw}(lt_{sw} + b1_{sw} + c1_{sw}) + \\
&ms2_{sw}(a1_{sw} + b1_{sw})(lt_{sw} + c1_{sw}) + \\
&mt2_{sw}(a2_{sw} + b2_{sw})(ls_{sw} + c2_{sw}) + \\
&mt1_{sw}a2_{sw}a2_{sw}(ls_{sw} + b2_{sw} + c2_{sw})]
\end{aligned} \tag{3.58}
$$

$$
Q_{21}^{-} = Q_{12}^{-} \tag{3.59}
$$

$$
Q_{22}^{-} = 0 \tag{3.60}
$$

$$
Q^{+} = \begin{bmatrix} Q_{11}^{+} & Q_{12}^{+} \\ Q_{12}^{+} & Q_{22}^{+} \end{bmatrix} \tag{3.61}
$$

$$
Q^{-} = \begin{bmatrix} Q_{11}^{-} & Q_{12}^{-} \\ Q_{12}^{-} & Q_{22}^{-} \end{bmatrix} \tag{3.62}
$$

3.3 Nine Mass Model Results

The nine mass model was derived to make a more versatile and adaptable model to better simulate the mass distribution throughout each limb, but do the extra four masses make a significant difference over the five mass model? To answer this question, I started by changing the moment of inertia of the shank and thigh on the right leg only while keeping the center of mass constant. This was done by moving the two masses an equal distance away from the center of the specific link (the shank and the thigh). A large asymmetry arose from changing the moment of inertia and keeping the center of mass constant on the right leg. I then corrected this asymmetry by changing both the moment of inertia and the

center of mass together on the left leg. Using the data from these tests, I was able to look at the trends of changing moment of inertia on a passive dynamic walker model. All of the masses, locations for the masses, and initial conditions are from [1].

The nine mass model can be used to model specific parts of a leg more accurately than the five mass model. This attribute will be seen later when the prosthetic model is discussed. In this test one of the legs is divided into four specific parts each described by its own mass and location. These parts could not have been described by the five mass model due to its lack of the necessary parameters. Also, the nine mass model is useful when testing correcting gait asymmetries by adding masses. This is shown later in this thesis where a large asymmetry is corrected by adding a mass to the thigh and shank. Adding a mass in the five mass model is not possible. The only way to create a similar test using the five mass model is to have the masses move along the links, but this does not describe the dynamics of adding a mass as accurately. A similar model to the nine mass model could have also been derived by taking the five mass model and adding moments to the links instead of added masses. I chose to derive the nine mass model because it would better describe the test previously mentioned than the five mass model with moments.

3.3.1 Creating a Large Asymmetry by Changing the Moment of Inertia While Keeping the Center of Mass Constant

To accomplish the task of changing the moment of inertia while keeping the center of mass constant, the parameter that separates the two masses on each link (i.e., $b1R$ and $b2R$) were incremented from 0m to 0.5m. Three tests were performed by incrementing $b1R$ and $b2R$ separately and both $b1R$ and $b2R$ simultaneously. This is done to change the moment of inertia while keeping the center of mass constant on the right leg. The goal of these tests was to find the largest asymmetry that arises, but still allow the PDW to walk successfully and have a stable gait. Step length difference is used in this research

to quantify asymmetry and it is a common way to describe asymmetry in human gait [17]. Similar to the five mass research, the walker configuration has to walk for fifty steps for a test to be successful. When the parameter that separates the two shank masses on the right leg ($b1R$) equals 0.24m, a step length difference of 0.0212m is generated. The asymmetry can be seen in Figure 3.4. For the test that separated the two thigh masses on the right leg, I found the largest asymmetry when $b2R = 0.25$m. This produces an asymmetry of 0.0297m and it can be seen in Figure 3.5. For the test when both $b1R$ and $b2R$ were changed simultaneously the largest asymmetry was 0.0300m. This asymmetry happens when $b1R = 0.07$ and $b2R = 0.26$ and can be seen in Figure 3.6. As already stated, these tests changed the moment of inertia while holding the center of mass constant. The reason I tested this is because the five mass system cannot change the moment of inertia without changing the center of mass. Figures 3.4 through 3.6 show the step length plot and the limit cycle trajectory plot. As discussed earlier, the step length plots show the step number versus step length and is a good measure of the symmetry of a walker configuration. The step length plots for Figures 3.4 and 3.5 are both single step patterns and the step length plot in Figure 3.4 is a double step pattern. The limit cycle plot depicts the angle versus the angular velocity in each phase of the model's gait for the right leg. Each color represents a phase in the dynamics following the right leg. Red and green are the three-link and two-link respectively while the right leg is swinging. After this, the right leg is the stance leg, where blue is the three-link and black is the two-link. By making these asymmetries, I have shown that changing the moment of inertia without changing the center of mass has direct implications on the gait dynamics. Figure 3.2 shows the nine mass model to reference the parameters that are discussed.

As a check to make sure the tests were done correctly. I took the largest asymmetries discussed earlier and repeated the same test but with the left leg to make sure the walker will have a symmetric gait when the parameters are symmetric. For example I took the asymmetry that arose when the masses on the thigh were separated by 0.25m and changed

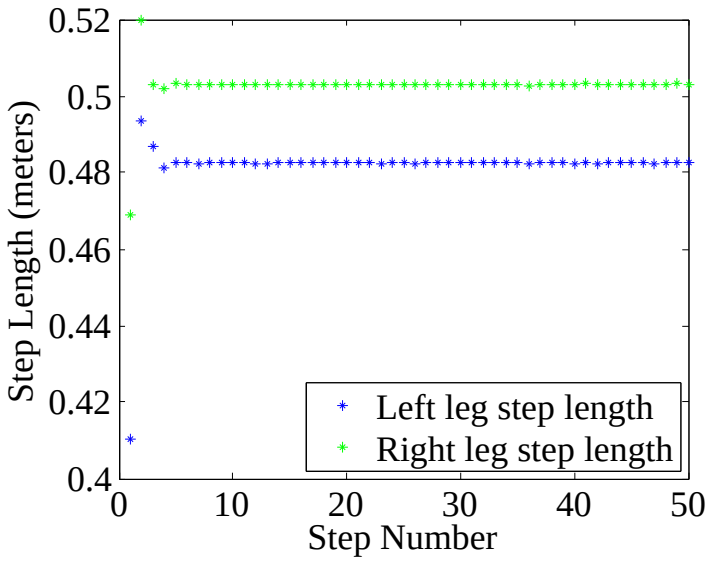

(a) The step length plot when $b1R = 0.24$m

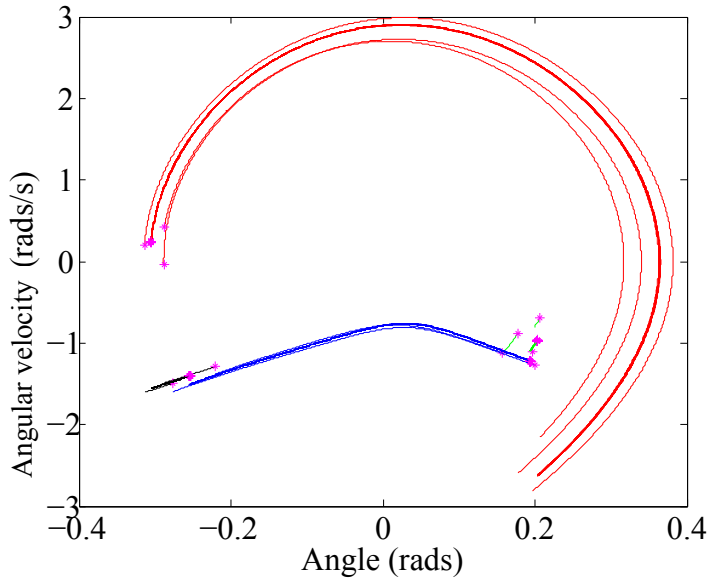

(b) The limit cycle plot when $b1R = 0.24$m

Figure 3.4: The masses on the right leg shank are separated by 0.24m. The separation of the shank masses results in an asymmetry of 0.0212m.

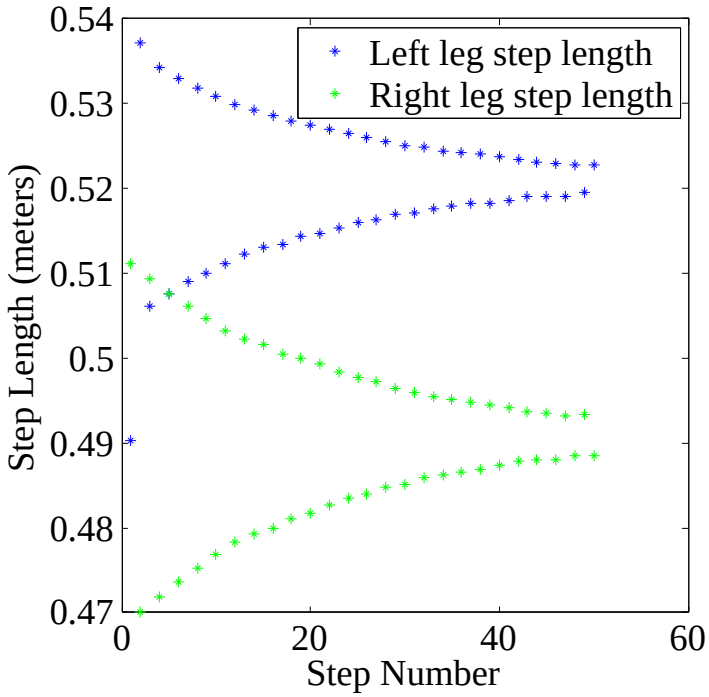

(a) The step length plot when $b2R = 0.25$m

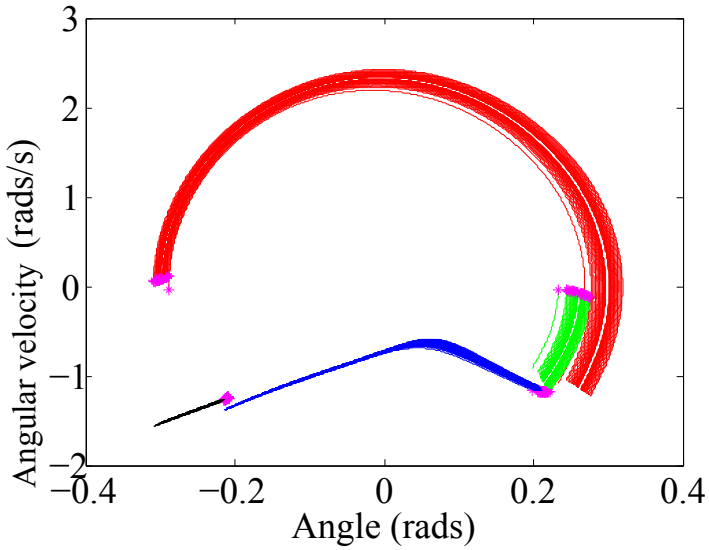

(b) The limit cycle plot when $b2R = 0.25$m

Figure 3.5: The masses on the right leg thigh separated by 0.25m. This results in an asymmetry of 0.0297m.

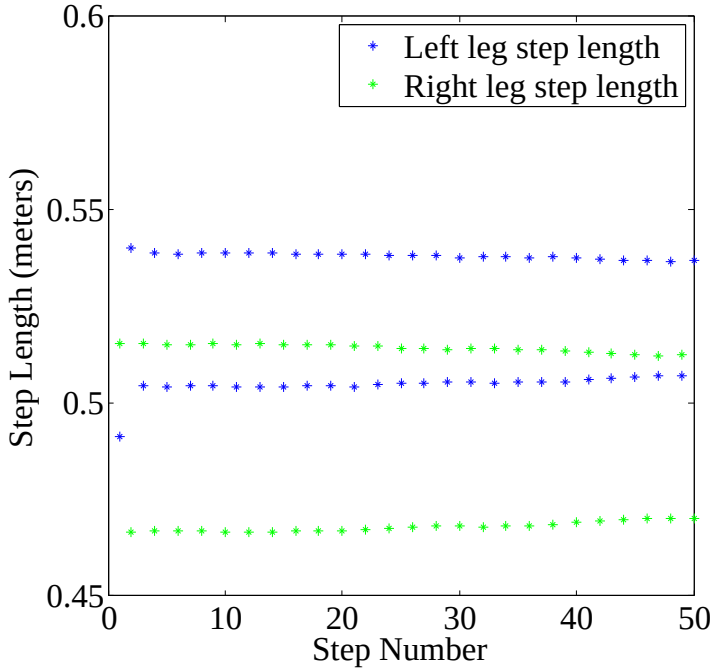

(a) The step length plot when $b1R = 0.07$m and $b2R = 0.26$m

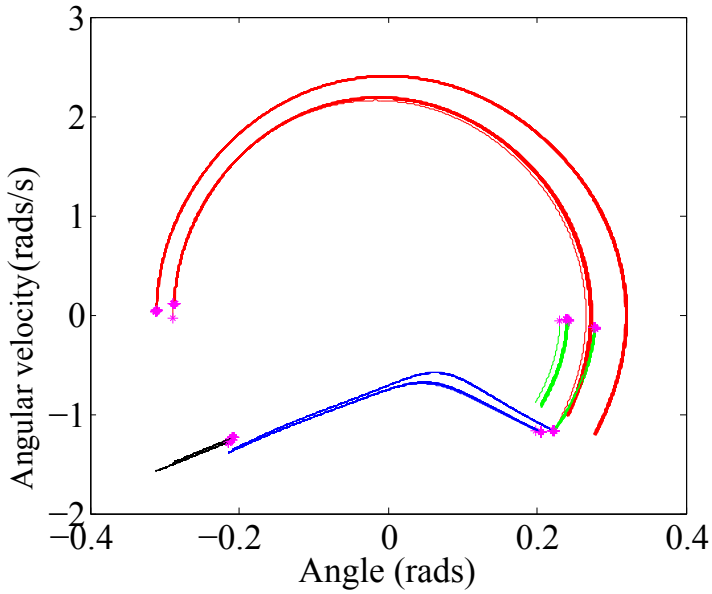

(b) The limit cycle plot when $b1R = 0.07$m and $b2R = 0.26$m

Figure 3.6: The masses on both the shank and thigh right leg are separated by 0.07m and 0.26m. This separation results in an asymmetry equaling 0.0300m.

the moment of inertia on the left leg thigh while holding the center of mass constant. I iterated through values of $b2L$ from 0m to 0.5m. This test had a symmetric gait pattern when $b2L = b2R = 0.25$m. This trend happened with all three testes. For the separated shank mass the model was symmetric when $b1L = b1R = 0.24$ and the same for when both the thigh and shank masses on the right leg were separated ($b1L = b1R = 0.07$m and $b2L = b2R = 0.26$m). This means that the data is valid because the model produces a symmetric gait when the parameters are symmetric.

3.3.2 Correcting the Large Asymmetries that Arose

Using the largest asymmetries from changing the moment of inertia on the right leg as a baseline, I tested the effect of changing the center of mass location on the left leg shank and thigh. Meaning, I am changing the center of mass on the leg opposite the leg I changed the moment of inertia on. The goal of this is to diminish the asymmetry that arose from changing the moment of inertia on the right leg by changing the center of mass on the left leg. The two masses on each link were moved on top of each other by setting $b1L$ and $b2L$ (see Figure 3.2) equal to zero. This effectively makes one large coupled mass on the left leg thigh and shank, making the left leg only have two masses on it. Now on the left leg the moment of inertia is dependent on the center of mass. This is unlike the previous test on the right leg where the center of mass remained constant while the moment of inertia changed.

I iterated through values of $c1L$ and $a2L$ from 0m to 0.5m with all permutations evaluated. The values of $a1L$ and $c2L$ were made dependent on $c1L$ and $a2L$ to maintain the total length for the shank and the thigh of 0.5m. There were walker configurations that resulted in having a symmetric gait pattern when the center of masses for the shank and thigh were at specific locations. Note that the left leg center of mass is changing which forces the moment of inertia to change because of the single coupled mass on

each link on the left leg. The goal of this test was to have a right leg and left leg with different moment of inertias but a symmetric gait. Figures 3.7 through 3.9 show the most symmetric solutions. Figure 3.7 shows the masses on the right leg shank are spread out by 0.24m. The walker model will go back to symmetry when the masses on the left leg thigh and shank are moved to 0.01m above the center of the center of the shank and thigh links. Comparing Figure 3.7 to Figure 3.4 the reduction of the asymmetric gait pattern is evident. The test with the largest asymmetry on the thigh ($b2R = 0.25$m) was able to achieve symmetry when the coupled mass on the left shank is moved 0.17m below the knee and the coupled thigh mass is moved to the center of the left thigh link (i.e. $a2L = 0.25$m). This symmetry is seen in Figure 3.8. Once again, comparing Figure 3.8 to Figure 3.5, it is clear that the asymmetry has been eliminated. Looking at Figure 3.9, it shows the symmetric solution to Figure 3.6. This symmetry occurs when the coupled thigh mass was moved to 0.23m below the hip and the coupled shank mass was moved to 0.14m below the knee. These tests show that when an asymmetry arises from changing the moment of inertia while keeping the center of mass constant on one leg, a symmetric gait can be achieved with a certain moment of inertia and center of mass on the opposite leg.

3.3.3 Trends of Changing Moment of Inertia on a Passive Dynamic Walker Model

Another interesting trend is how changing the moment of inertia on the left leg affects the step length difference when the right leg is held constant. Using the data obtained by changing $c1L$ and$a2L$ and holding the right leg constant with the link masses spread apart at a distance that produced the largest asymmetries, I plotted the moment of inertia for each leg versus the step length difference. Figures 3.10 through 3.12 shows both the moment of inertia of the left and right legs versus step length difference and the three dimensional plot of $a2L$ versus $c1L$ versus step length difference. Figure 3.10 occurs

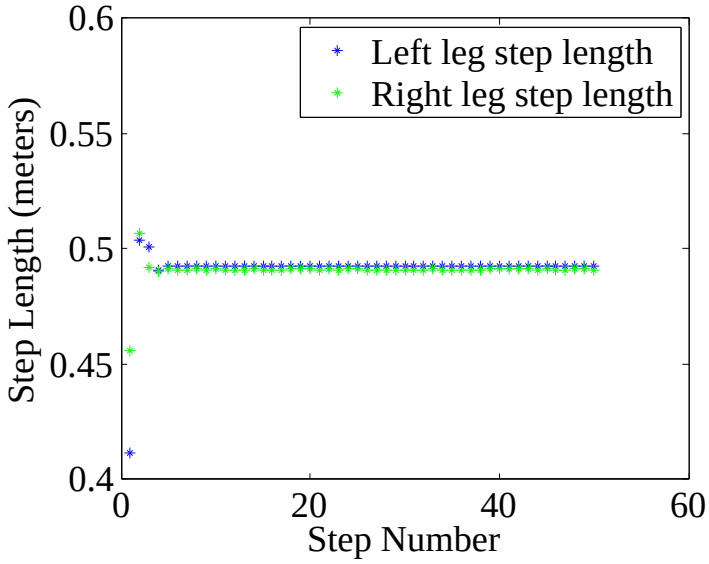

(a) Symmetric Step Length Plot

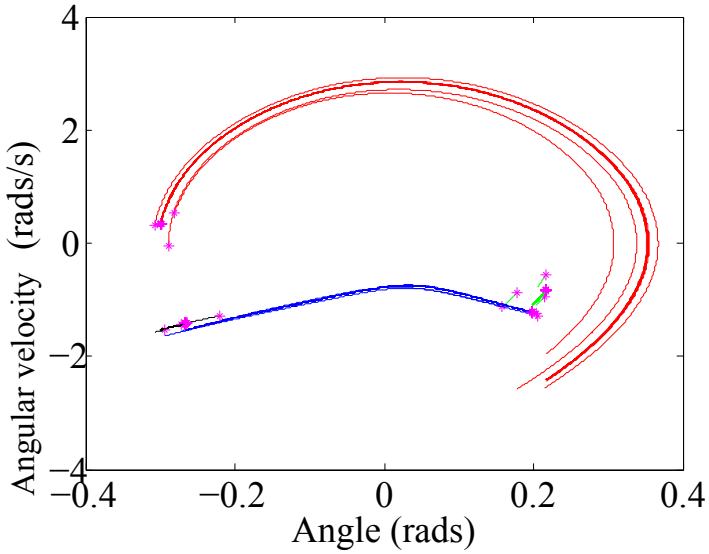

(b) Symmetric Limit Cycle Plot

Figure 3.7: The symmetric solution when the shank masses on the right leg are separated by 0.24m. This symmetry happens when the left leg thigh and shank masses are both positioned positioned at 0.01m above the center of the left leg shank and thigh respectively.

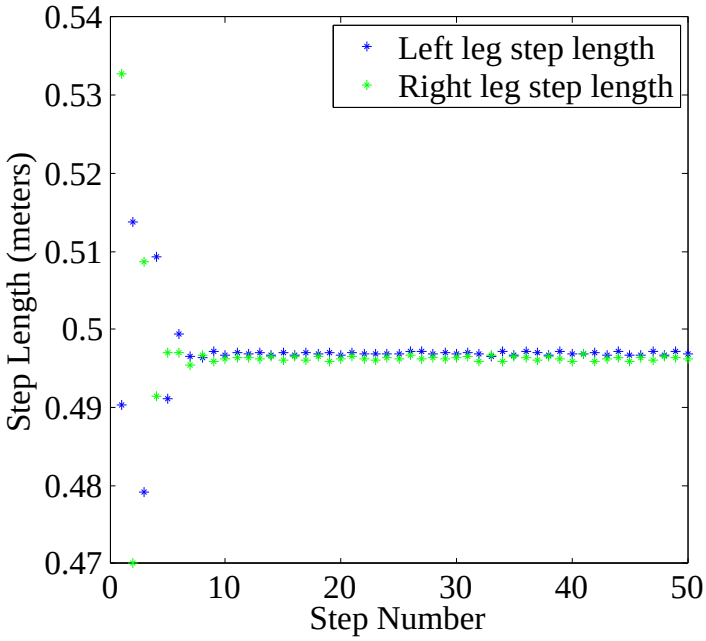

(a) Symmetric Step Length Plot

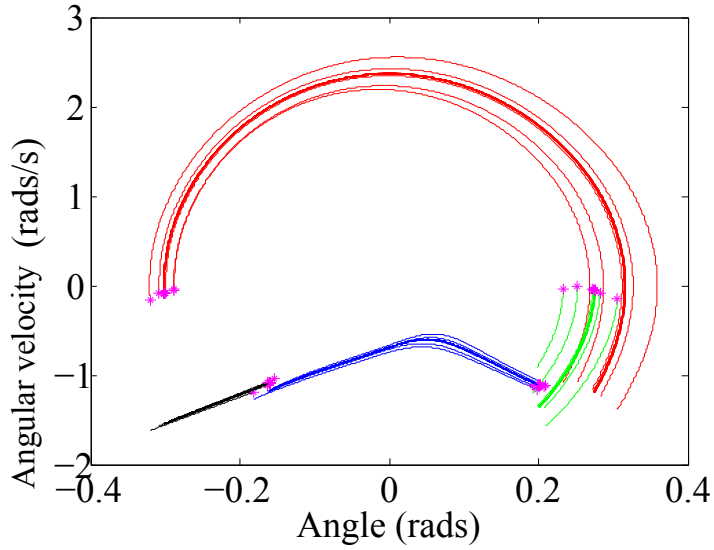

(b) Symmetric Limit Cycle Plot

Figure 3.8: The symmetric solution when the thigh masses on the right leg are separated by 0.25m. The symmetry occurs when the left leg shank mass is 0.17m below the knee and the thigh mass is moved to the center of the thigh ($a2L = 0.25$m)

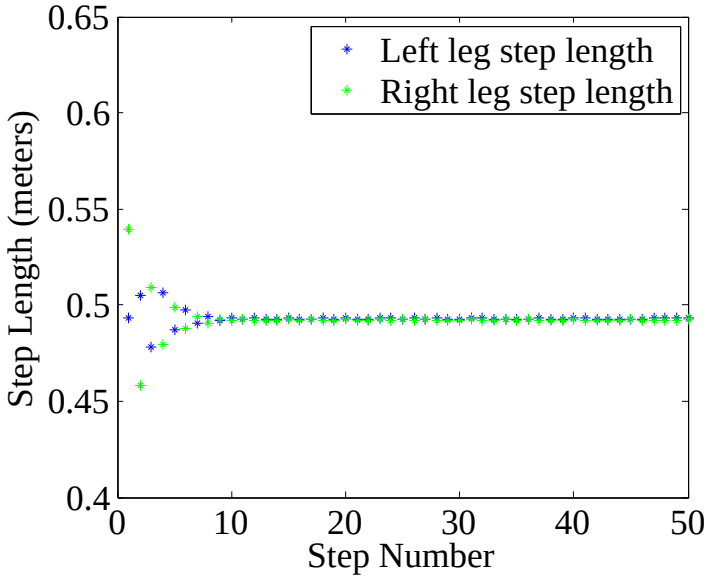

(a) Symmetric Step Length Plot

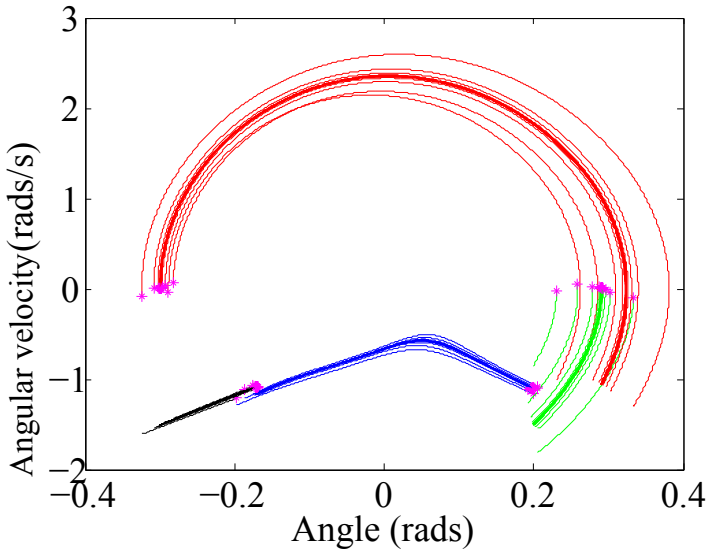

(b) Symmetric Limit Cycle Plot

Figure 3.9: The symmetric solution when the thigh masses on both the shank and thigh right leg are separated by 0.07m and 0.26m. This symmetry happens when the left leg shank mass is moved 0.14m below the knee and the thigh mass is moved 0.23m below the hip.

when the right leg shank masses are separated by 0.24m and the center of mass location is varied on the left leg. Figure 3.10a shows that as the moment of inertia of the left leg (black dots) approaches 0.04 the step length difference increases. The solid vertical red line is the constant moment of inertia of the right leg. An interesting result is when the moment of inertia for both legs are equal there is still an asymmetry. This shows that symmetric gait patterns rely both on center of mass and moment of inertia. Figure 3.10b shows how $c1L$ and $a2L$ affect the step length difference when $b1R = 0.24$m. Looking at Figure 3.11, this is when the right leg thigh masses are spread by 0.25m and $c1L$ and $a2L$ are changing. Figure 3.11a is the moment of inertia of the left leg (black dots) versus the step length difference. As seen in this figure, the moment of inertia of the left leg is dependent on the location of mass. The location of the thigh and shank masses change with $c1L$ and $a2L$,which is depicted by the colored lines in Figure 3.11a. The green line in Figure 3.11a shows when $c1L = 0.25$. At some instances when $c1L = 0.25$, the model is very symmetric but as $a2L$ increases the model becomes more asymmetric. Figure 3.11b is the three dimensional plot of $a1L$ versus $c2L$ versus. step length difference. It shows that there are a range of values of $a1L$ and $c2L$ that produce a symmetric gait pattern given an altered moment of inertia. Figure 3.12 shows similar plots as Figure 3.11, but the right leg shank and thigh mass are both spread out by 0.07m and 0.26m respectively while still $c1L$ and $a2L$ are changed. All of these plots show that changing the moment of inertia has a distinct impact on the symmetry of the walker.

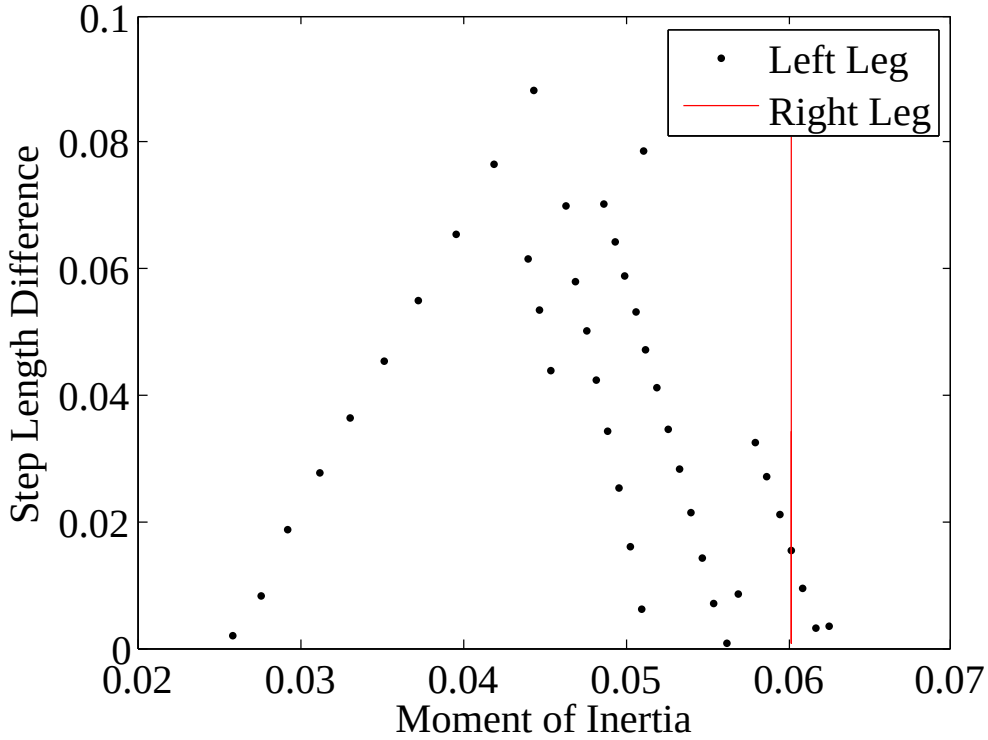

(a) Moment of inertia of the left leg when the right leg shank mass is spread out by 0.24m.

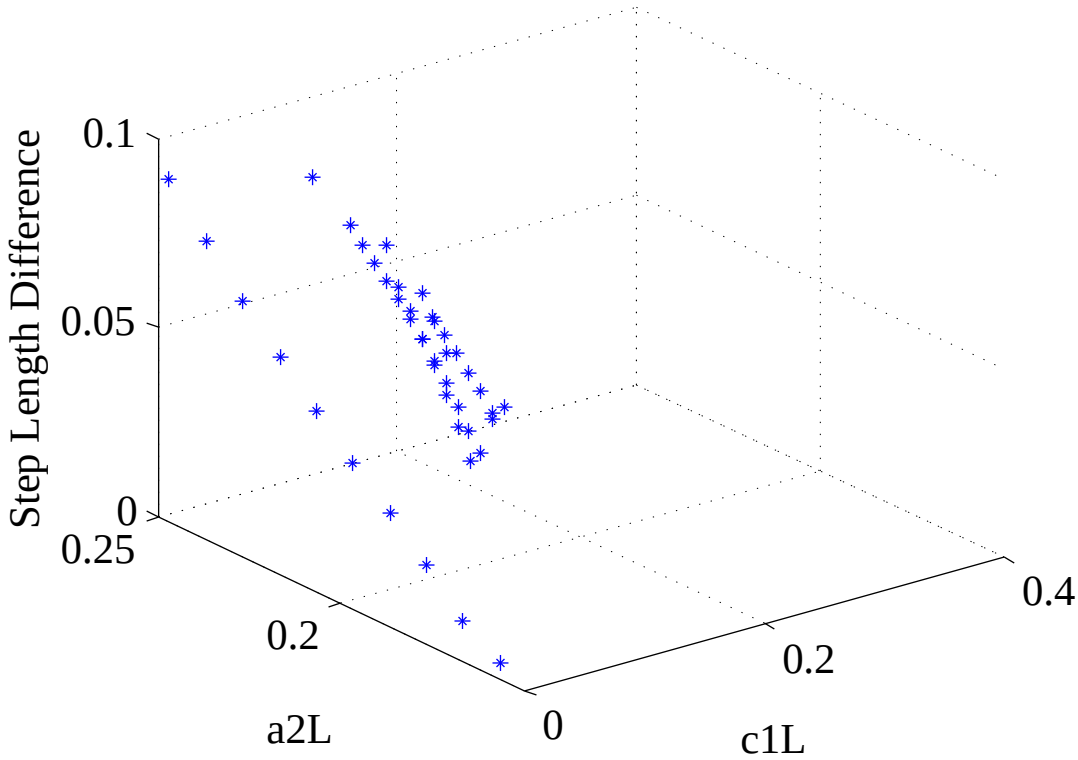

(b) a2l and c1L versus Step Length Difference

Figure 3.10: The step length changing with different parameters when $b1R = 0.24$m.

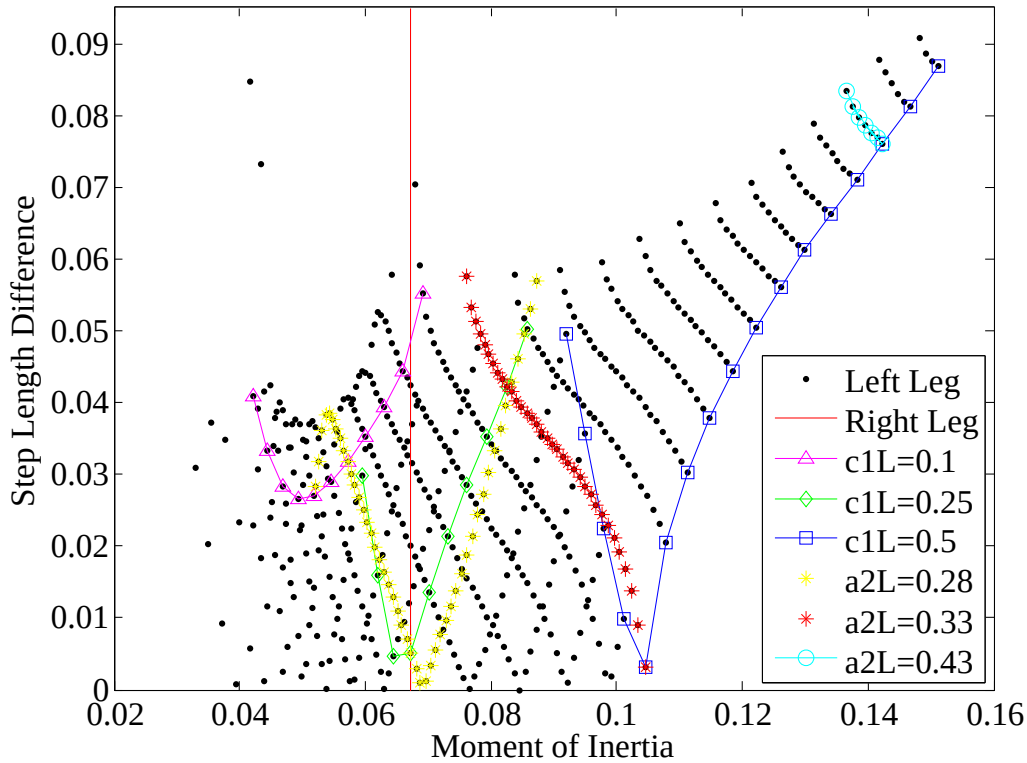

(a) Moment of inertia of the left leg when the right leg thigh mass is spread out by 0.25m.

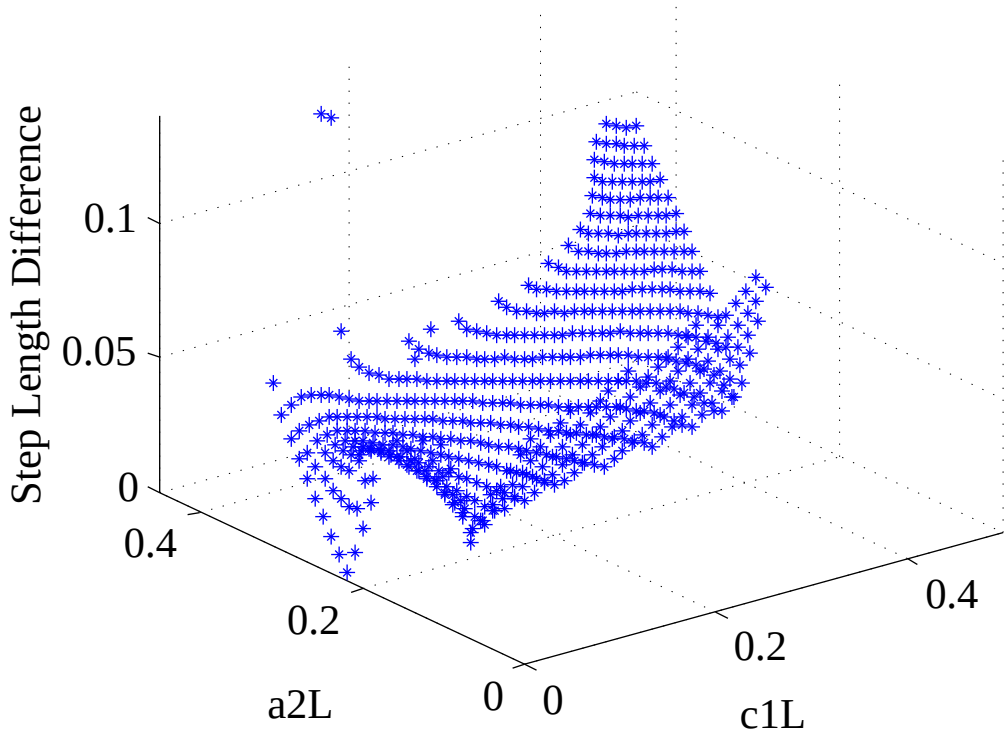

(b) a2l and c1L versus Step Length Difference

Figure 3.11: The step length changing with different parameters when $b2R = 0.25$m.

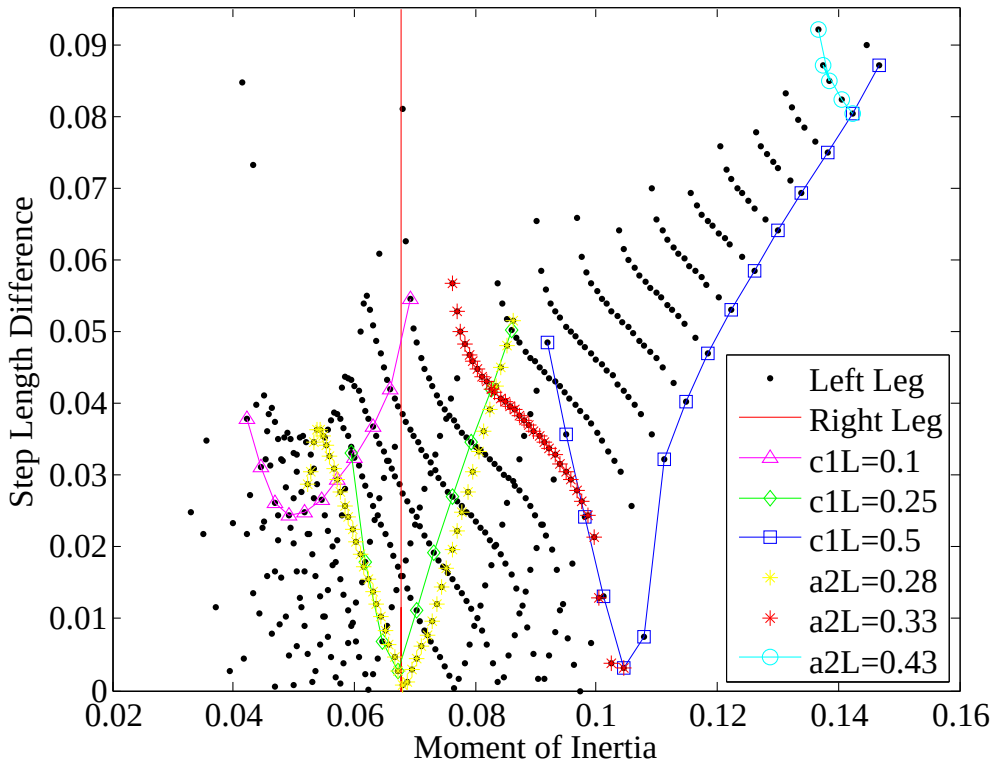

(a) Moment of inertia of the left leg when the right leg shank and thigh mass are both spread out by 0.07m and 0.26m respectively.

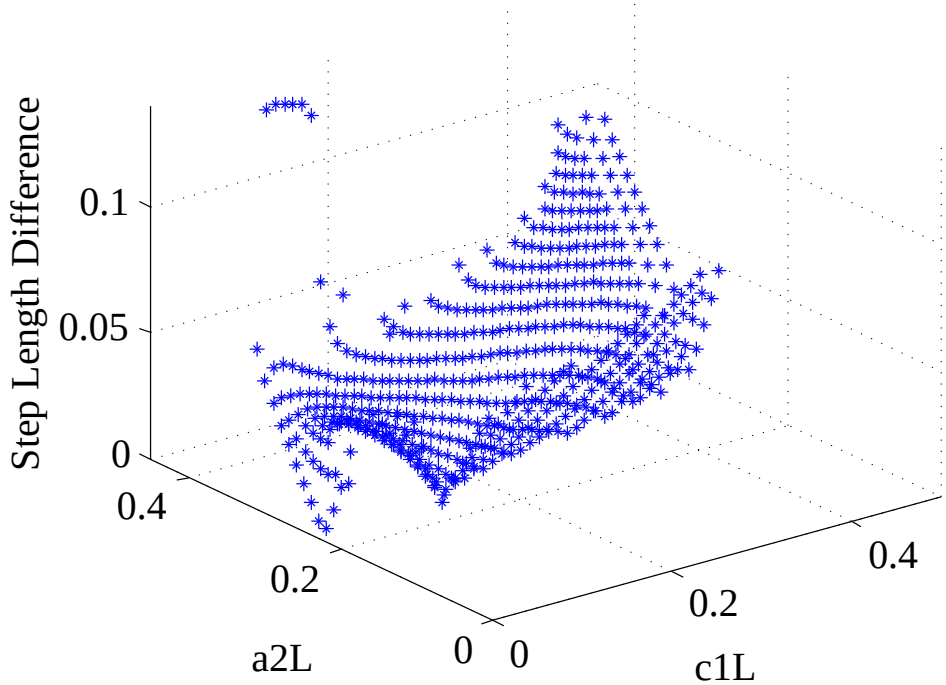

(b) a2l and c1L versus Step Length Difference

Figure 3.12: The step length changing with different parameters when $b1R = 0.07$m and $b2R = 0.26$m.

Chapter 4: Model Uses

The nine mass model can be applied to many applications. An interesting application I found was to correct the asymmetry that emerges from having one leg longer than the other by adding two masses to the opposite shank and thigh at a specific location. I also created a model that is anatomically correct by comparing the nine mass model to human anthropomorphism. Using this anthropomorphic model, I looked at prosthesis design and created a theoretical transfemoral prosthetic limb. This prosthetic is lighter and produces a more symmetric gait pattern than today's prostheses. The nine mass model is also being used to design and tune a physical passive dynamic walker. These are just some of the applications I have worked with to date. The possibilities are endless with what this model could be applied to, especially in the field of gait rehabilitation.

4.1 Correcting a Longer Leg's Asymmetry by Adding Mass

The nine mass model has the ability to vary a large amount of parameters. I used this ability to test if the natural asymmetry that arises from having one leg longer than the other can be diminished by adding a mass to the shank and thigh. From [11], I found that having one leg significantly longer than the other produces a very large asymmetry. The goal of this test is to reduce the asymmetry by adding a changing mass with changing position on the opposite shank and thigh. To create this test I had to change five different parameters, which is more than any other test described in this thesis. In this test, I made the right leg range from the original length of 1m to 1.05m. To correct the asymmetry

that arises, I started with the five mass system and used the extra two masses ($ms2L$ and $mt2L$) on the left leg as added gait correcting masses. The magnitude and location was changed for the added masses on the left leg, making for five different parameters changing. The magnitudes range from 0 to 25% of the normal shank and thigh mass. The location of each mass spans the whole length of the individual link. Once again, a walker configuration was considered successful if it was able to walk fifty steps.

This test produced an abundance of interesting gait data. For one, 99.3% of the passing walking configurations had the added thigh mass ($mt2L$) equaling 0.025kg. This is because the mass of the thigh has a large effect on the symmetry of the walker [11]. Figure 4.1 shows holding $mt2L$ constant at 0.025kg and plots the length of the right leg versus the step length difference. An interesting trend in this figure is when the right leg is 1.03m or less, the walker is able to achieve a symmetric gait.

There were two different leg lengths I was interested in, when the right leg is the longest ($LR = 1.05$m) and when $LR = 1.02$m. I chose $LR = 1.02$m because it has many symmetric solutions (Figure 4.1) while still maintaining a right leg that is noticeably

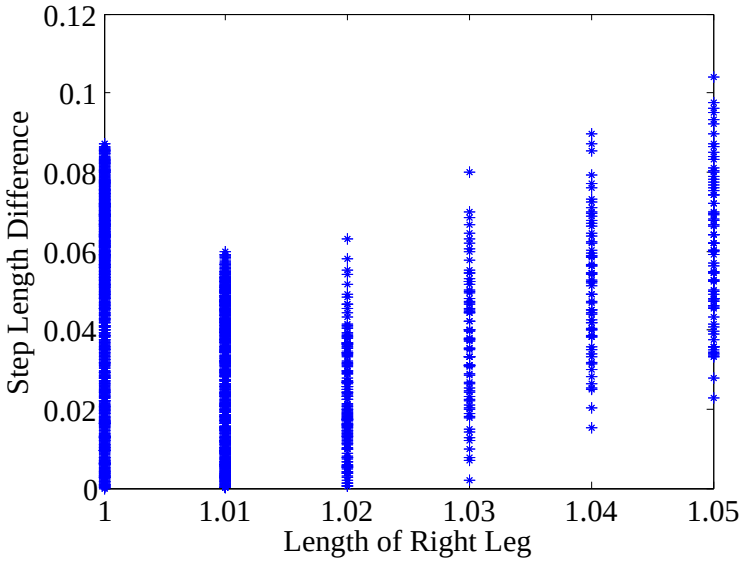

Figure 4.1: The plot of $mt2L$ versus step length.

longer than the left leg. When looking at Figure 4.1, it can be seen that a right leg equaling 1.05m does not have any symmetric configurations but has some that are very close.

Figure 4.2a shows $ms2L$ versus step length when the right leg is 1.02m long. For all values in this plot $mt2L$ is constant at 0.025kg. It is apparent that the step length changes with another parameter besides $ms2L$. In Figure 4.2b, $b1L$ versus $b2L$ versus step length is plotted. This shows how changing the locations of the masses affects the symmetry of the model. A trend for this plot is that the position of the added thigh mass ($b2L$) has a large effect on the step length difference. For values of $b2L$ below 0.2m the model is symmetric for the whole range of values for $b1L$. The most symmetric solution for a $LR = 1.02$ occurs when $mt2L = 0.025$kg, $b2L = 0.25$m, $ms2L = 0.0025$kg, and $b1L = 0.1$m. Conceptually, this means that the added thigh mass is directly on top of the knee. The symmetry for this configuration can be seen in Figure 4.3. The step length plot is seen in Figure 4.3a and the limit cycle plot is seen in Figure 4.3b. When looking at Figure 4.2b, there is one configuration that has the largest asymmetry. Interestingly the largest asymmetry and the smallest asymmetry have the same location of the added thigh mass ($b2L = 0.25$m), with the mass directly on top of the knee. Over 13% of all passing configurations exhibit this trait of having $b2L$ equaling 0.25m. The added mass on the shank increased from the symmetric configuration ($ms2L = 0.0025$kg) to the most asymmetric ($ms2L = 0.01$kg) and the location of the mass moved down to the bottom of the shank, creating a foot mass. This asymmetry can be seen in Figure 4.4.

When the right leg is 1.05m, the model does not exhibit many stable gait patterns. This is because having a leg 0.05m longer than the other leg develops a very large asymmetry and the changing parameters on the shorter leg does not have a large enough effect to overcome the asymmetry. I could have varied more parameters like adding weights to the longer leg and changing the hip mass. This could be something interesting to analyze in the future.

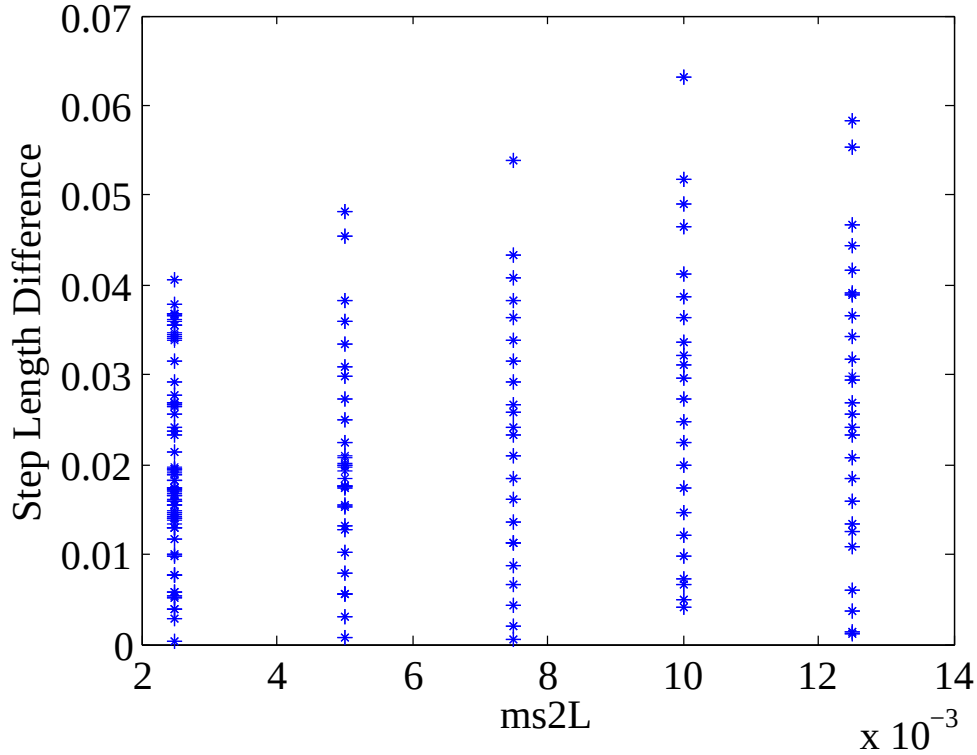

(a) This figure shows the $ms2L$ versus step length difference.

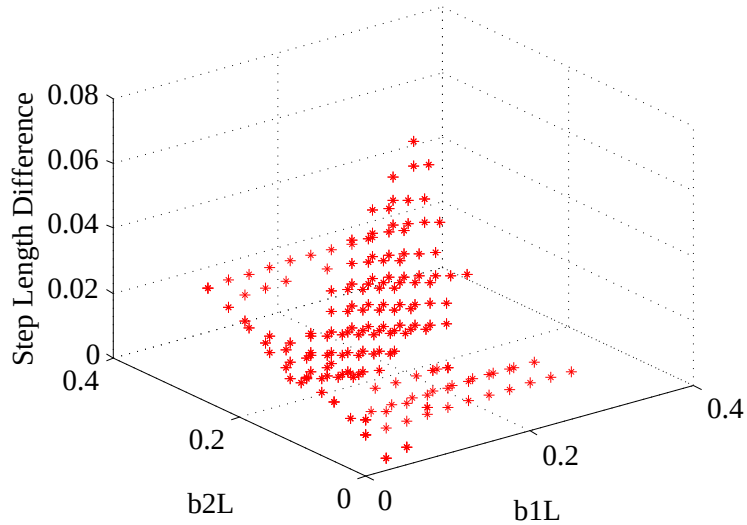

(b) This figure $b1L$ versus $b2L$ versus step length.

Figure 4.2: This plot shows the gait dynamics when the right leg is 1.02m long.

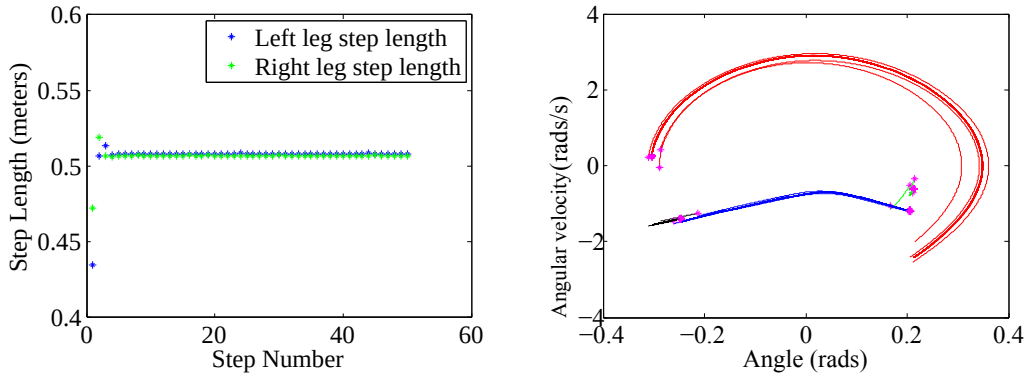

(a) The step length plot when the right leg is 1.02m.

(b) The limit cycle plot when the right leg is 1.02m.

Figure 4.3: The symmetric solution when the right leg is 1.02m. This happens by adding a mass on the left leg shank and thigh with a magnitude of 0.0025kg and 0.025kg respectively. The mass on the thigh is located on the knee ($b2L = 0.25$m) and the shank mass is 0.1m above the center of the shank

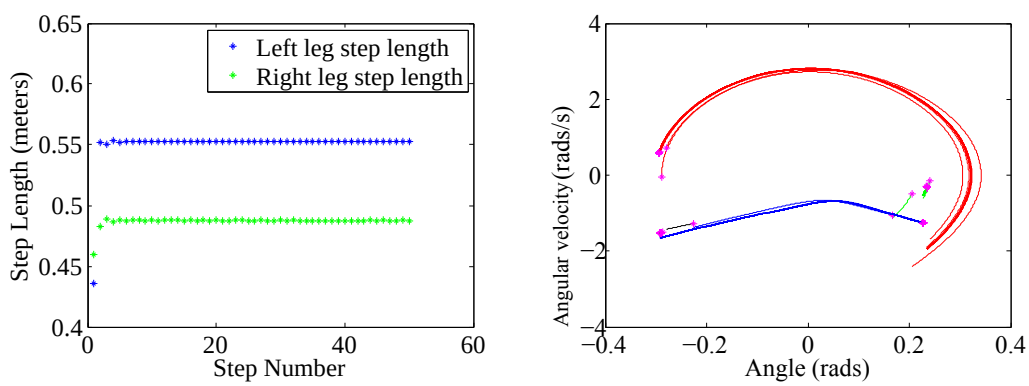

(a) The step length plot when the right leg is 1.02m.

(b) The limit cycle plot when the right leg is 1.02m.

Figure 4.4: The configuration with the largest asymmetry when the right leg is 1.02m. This asymmetry arises when the thigh and shank mass on the left leg are 0.025kg and 0.01kg respectively. The thigh mass stays on the knee and the shank mass moves down to the bottom of the shank, creating a foot mass.

Figure 4.5a shows $ms2L$ versus step length difference. Similar to when $LR = 1.02$m, this plot shows $LR = 1.05$m and holds $mt2L$ constant at 0.025kg, because $mt2L$ does not change for all passing values when $LR = 1.05$m. It can also be seen in Figure 4.5a that the step length is being changed by another parameter besides $ms2L$. Figure 4.5b plots $b1L$ versus $b2L$ versus step length. In this plot there is a line that has a $b2L = 0$m and a changing $b1L$, all with very low asymmetries. There is also a large gap between the line of symmetry and the rest of the working configurations; between $b2L$ of 0m to 0.175m, there are no working configurations. This is due to the fact that the thigh is very sensitive to added mass, especially in the middle of the link [11]. So the added thigh mass creates a passing configuration when it is located at the extremes of the thigh, at the hip or close to the knee. Also, Figure 4.5b shows how the value of $b1L$ drives the symmetry and success of the walker. When $b2L$ is approximately 0.25m and $b1L$ is small, the model has a small asymmetry, but as $b1L$ increases the asymmetry increases. The most symmetric solution occurs when the added thigh mass ($mt2L$) is 0.025kg, it is located at the center of the link ($b2L = 0.00$m), the added shank mass ($ms2L$) is 0.0025kg, and it is located 0.1m below the knee ($b1L = 0.15$m). Figure 4.6 shows the asymmetry and gait dynamics for the smallest asymmetry when $LR = 1.05$m. In Figure 4.5b, the largest asymmetry occurs when $mt2L = 0.025$kg, $b2L = 0.25$m, $ms2L = 0.01$kg, and $b1L = 0.2$m. This asymmetry is seen in Figure 4.7. With a right leg length of 1.05m, the model cannot produce a symmetric gait, but with the parameters changing the model can come close to symmetry.

This test showed that the asymmetry from having one leg longer than the other can be reduced. The results from this test will do nothing to align the joints of an individual with one leg that is longer than the other. However, the ability to reduce the natural asymmetry will help alleviate joint pain and the energy used while walking [20][14]. I was able to find symmetric solutions to a leg that is 0.03m longer than the normal leg. A leg that is 0.03m longer than the normal leg is significant and would be a large impairment for an

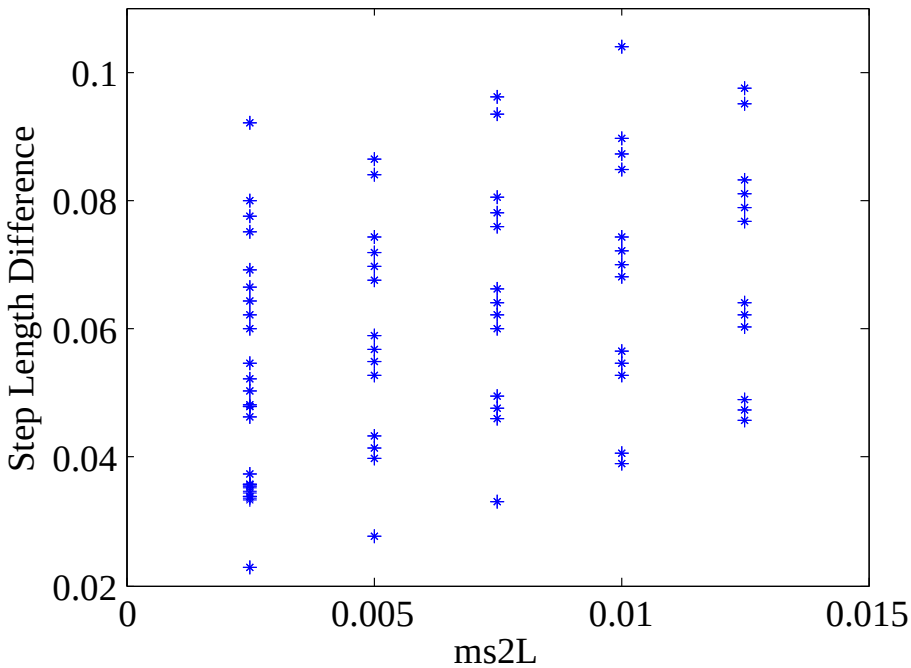

(a) This figure shows the $ms2L$ versus step length difference.

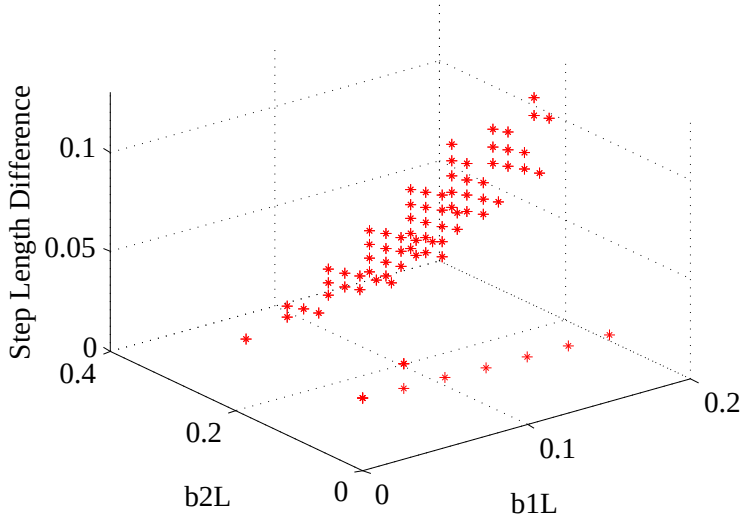

(b) This figure $b1L$ versus $b2L$ versus step length.

Figure 4.5: These plots show the gait dynamics when the right leg is 1.05m long.

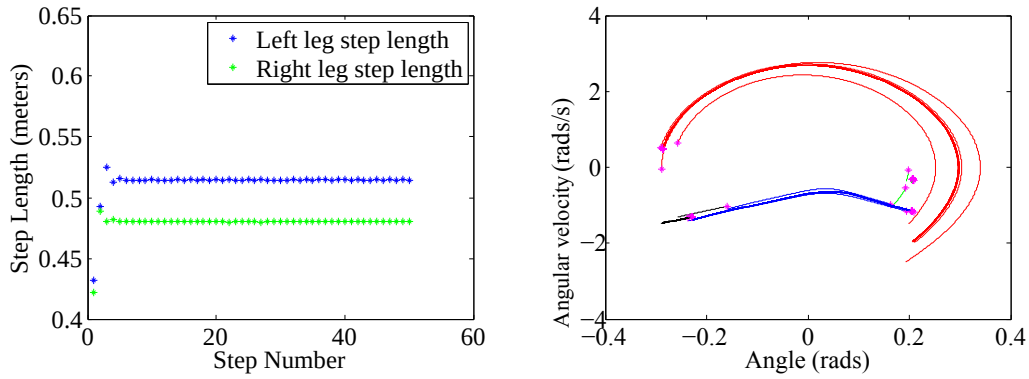

(a) The step length plot when the right leg is 1.05m.

(b) The limit cycle plot when the right leg is 1.05m.

Figure 4.6: The symmetric solution when the right leg is 1.05m. The most symmetric solution happens when the left leg has a thigh mass equaling 0.025kg and is located at the center of the thigh and has a shank mass of 0.0025kg and is located 0.1m below the knee.

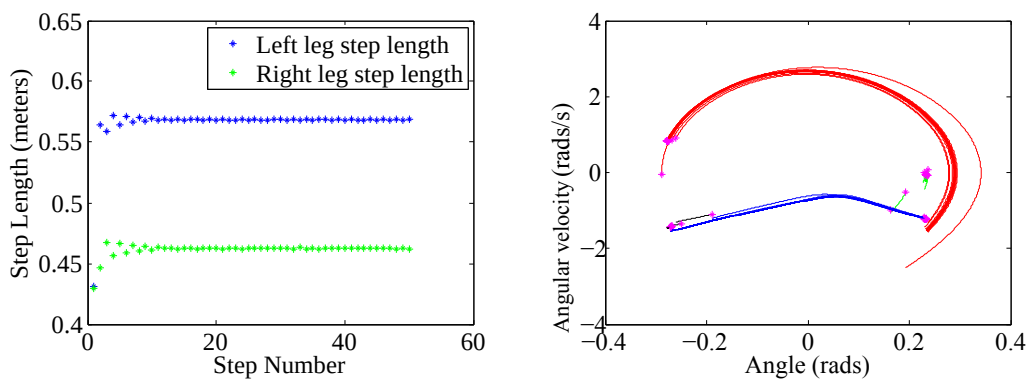

(a) The step length plot when the right leg is 1.05m.

(b) The limit cycle plot when the right leg is 1.05m.

Figure 4.7: The configuration with the largest asymmetry when the right leg is 1.05m. This large asymmetry occurs when the left leg thigh mass is 0.025kg and the shank mass is 0.01kg. The thigh mass is at the knee and the shank mass is located at 0.05m above the bottom of the shank

individual with such a problem. As interesting as this data is, it still can be improved by changing more parameters and having the initial parameter conditions be anatomically correct.

4.2 Anthropomorphic Model

To better describe the human gait and test rehabilitation methods, I have derived an anthropomorphic model based upon the nine mass model. Figure 4.8 shows the mass locations for the anthropomorphic model. It is essentially a seven mass model because I coupled the two thigh masses into one large mass. To create this model, I used human anthropomorphic data found in [5]. I took the values given in the anthropomorphic data and varied them until I found a symmetric gait pattern. The values for the given anthropomorphic masses and the derived model masses are in Table 4.1. It can be seen that the two masses that needed to be changed to achieve symmetry are the mass of the thigh and the mass of the shank. Table 4.2 shows the location of each mass. The first column is the given mass location from the anthropomorphic data. It describes the center of mass location from the proximal endpoint. This is where the center of mass is located on the current link from the center of mass on the link before. The second column is the calculated length for the walker and the third column is the mass location on the walker. Note that the calculated length for the hip is zero because it does not have a distance from a previous link, it is located at the top of the walker. Also, the position of the foot is not based on the anthropomorphic data. It is placed at the bottom of the walker and the length to the foot is the length of the shank minus the length of the shank mass location ($0.285 = 0.5\text{m} - 0.2165\text{m}$). This model was created to aid in the testing of rehabilitation methods.

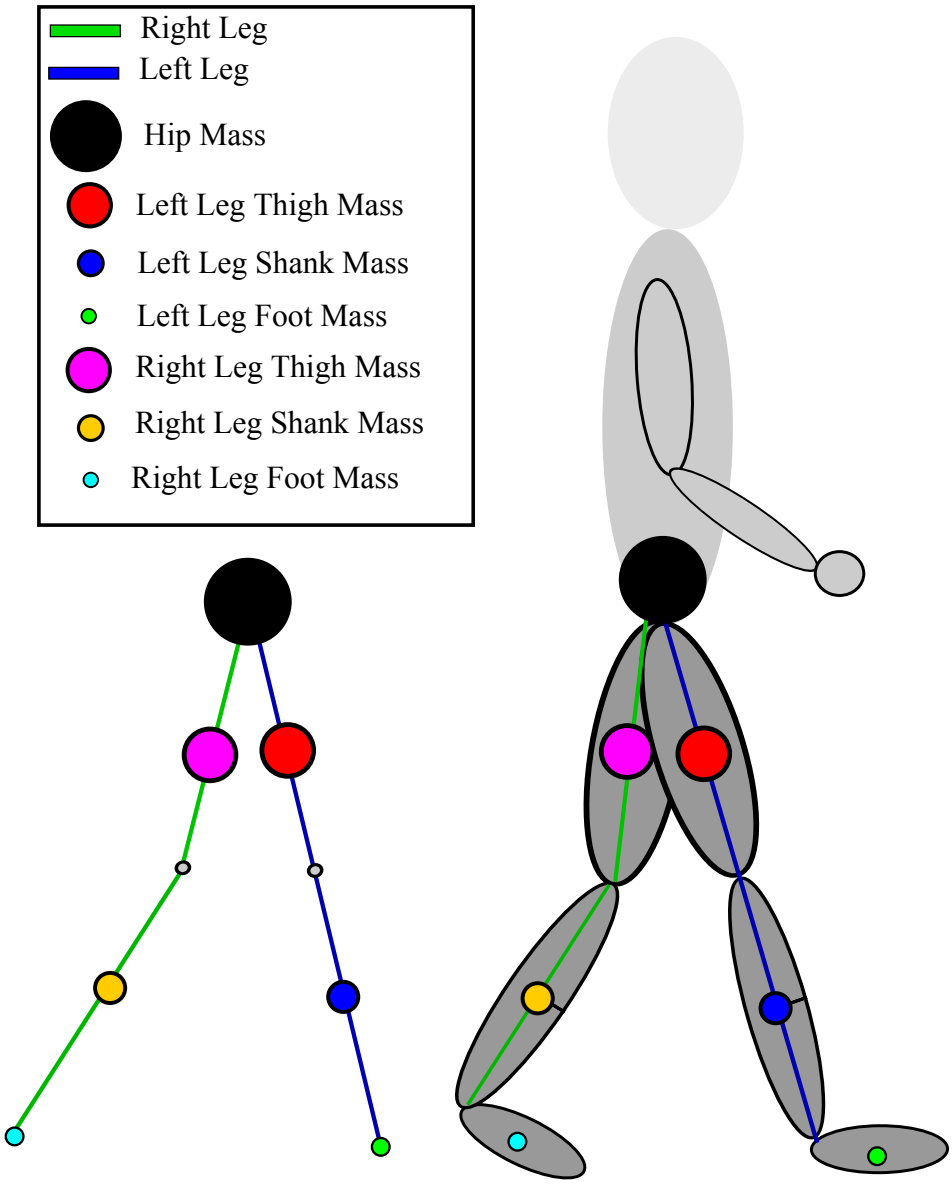

Figure 4.8: The anthropomorphic model. This shows the anthropomorphic model that was derived to better represent human leg mass.

Table 4.1: Anthropomorphic Model Mass

	Mass of Hip (kg)	Mass of Thigh (kg)	Mass of Shank (kg)	Mass of Foot (kg)
Given Masses	0.532	0.115	0.044	0.019
Derived Model	0.532	0.315	0.1	0.019

Table 4.2: Anthropomorphic Model Mass Locations

Walker Parameter	Center of Mass Location From Proximal Endpoint	Calculated Length (m)	Model Location
Hip	0.54	0	At Top of Walker
Thigh	0.433	0.2165	From Hip
Shank	0.433	0.2165	From Knee
Foot	0.429	0.2385	From Shank Location

4.3 Prosthetic Model

Using the anthropomorphic model, I derived a theoretical transfemoral prosthetic limb. I assumed that one third of the thigh has been removed above the knee. This makes the stump mass two thirds the mass of the intact thigh and it is also two thirds of the length. In the model, the prosthetic thigh and shank both have changing masses and lengths to find the optimal values for the knee location, prosthetic shank mass, prosthetic thigh mass, and a symmetric gait. The intact leg is exactly the same as the anthropomorphic model. Figure 4.9 shows the prosthesis model with the mass locations. The model has one thigh mass representing the center of mass of the stump mass and the other thigh mass representing the center of mass for the prosthetic thigh. Even though the length of the prosthetic thigh changes, the model is set up to keep the mass in the center for every iteration. A point mass on the shank was used to represent the prosthetic shank center of mass. Once again the model was set up to keep the mass at the center of the shank with the changing length of the shank. The foot mass is represented by a point mass on the bottom of the model prosthetic limb. Looking at Figure 4.9, the masses are from top

to bottom: dark grey represents the stump mass, red is the prosthetic thigh, green is the prosthetic shank, and blue is the prosthetic foot. Also, notice how the knee line for the intact leg and prosthetic leg differ.

4.3.1 Prosthetic Model Results

This model of a transfemoral prosthesis is used in this thesis to break the assumption that the prosthetic knee location should be located in the same location as the existing knee. Here, I describe three different prosthetic model configurations. The first is a baseline where the intact knee and prosthetic knee are in the same location. For the model to walk symmetrically, the total mass of the prosthetic leg had to increase by 2%. For this 2% leg mass increase, the prosthetic thigh increased by 17% and the prosthetic shank decreased by 38%. This data is shown in the first row of both Tables 4.3 and 4.4 and the symmetry can be seen in Figure 4.10. For the second test, I was able to achieve a stable symmetric gait when the prosthetic knee was moved down by 36.7% in relation to the intact knee. In doing this I reduced the prosthetic shank mass by 68% and the prosthetic thigh mass increased by 7.3%. This resulted in a total mass reduction of 13.4%. The results from this test can be seen in the second row of both Tables 4.3 and 4.4 and the symmetry in Figure 4.12. Even though 13.4% total mass reduction is not dramatic, the prosthetic shank mass decreased drastically. Mattes et al. discuss that lowering the mass prosthetic shank is very important for energy cost reduction [14].

Individuals who wear prostheses commonly have an asymmetry where their prosthetic leg has a longer step length than their intact leg [14]. The first two tests have shown that a symmetric gait can be achieved with a transfemoral prosthesis when either the weight is increased or more importantly the knee is moved. For the third test, I went past the normal asymmetry of a prosthesis where a prosthetic leg has a longer step length than the intact leg to make the prosthetic leg have a shorter step length than the intact leg. This

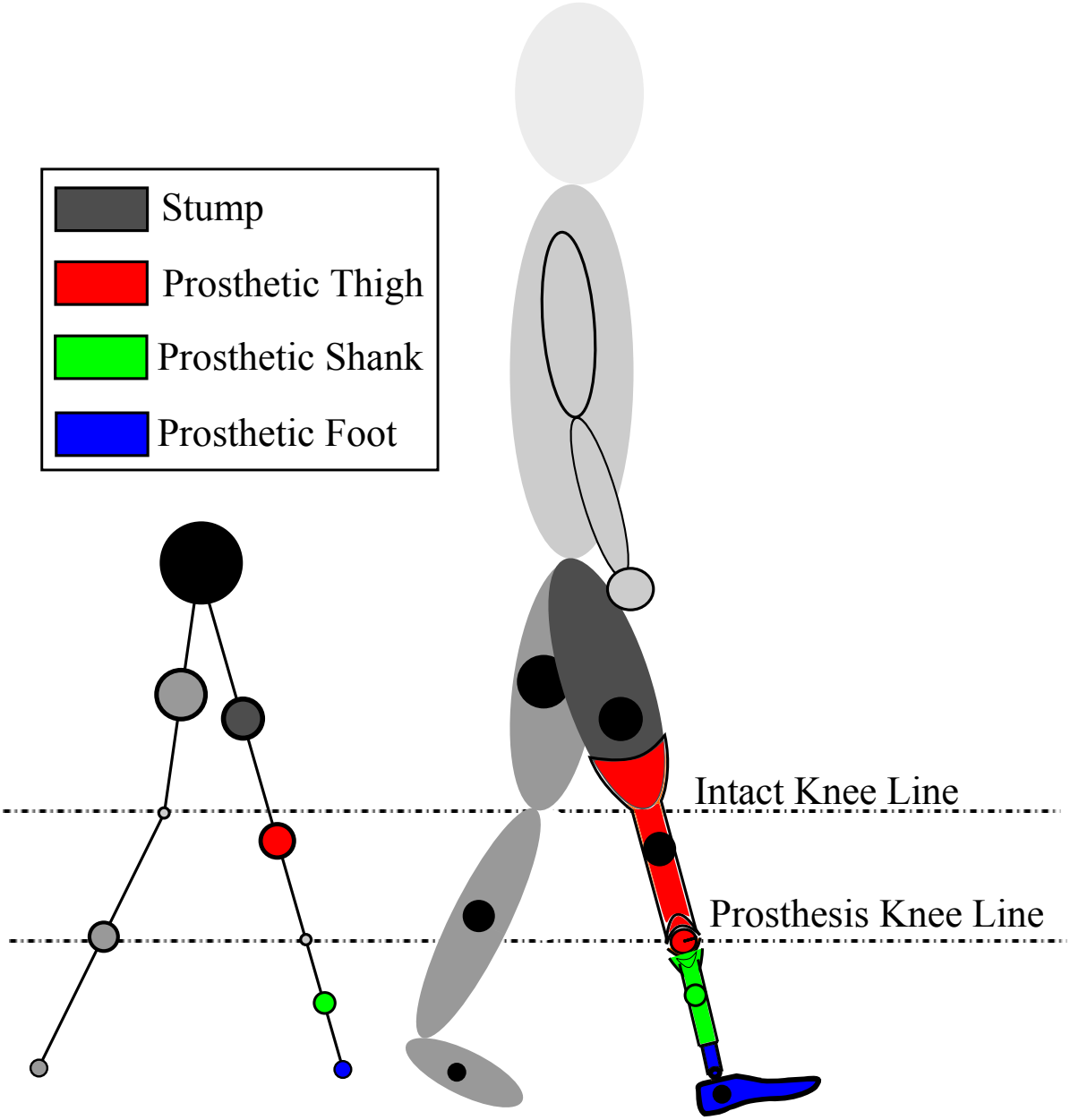

Figure 4.9: The prosthesis model. This shows the prosthesis model that was derived to better represent a transfemoral prosthetic leg.

configuration would mean that the prosthetic leg is overcompensating for the asymmetry that the wearer of the prosthesis is likely to develop. To get this gait pattern the knee had to be moved down by 42.8% in relation to the intact knee. This caused a 63% mass reduction in the prosthetic shank and 2% reduction in the prosthetic thigh mass, giving a total prosthesis mass reduction of 19%. The results in the third test can be seen in the third row of both Tables 4.3 and 4.4 and the asymmetry in Figure 4.12. This test shows that the model can theoretically tune a prosthetic leg to be lighter than the intact leg while overcompensating for the wearer's developed asymmetry.

Table 4.3: Prosthesis Model Mass Results

Configuration	Thigh Mass Change	Shank Mass Change	Total Mass Change
Heavier Symmetric	17% increase	38% decrease	2% increase
Lighter Symmetric	7.3% increase	68% decrease	13.4% decrease
Lighter Asymmetric	2% decrease	63% decrease	19% decrease

Table 4.4: Prosthesis Model Knee Location Results

Walker Configuration	Knee Location Change
Heavier Symmetric	0
Lighter Symmetric	36.7% down
Lighter Asymmetric	42.8% down

4.4 Physical Walker

The nine mass model can also be used to design and tune a physical passive dynamic walker (PDW). In [10] there is research being done to create the physical PDW seen in Figure 4.13. The nine mass model has aided in the design and tuning of the PDW. To use the nine mass model for design and tuning, a model that describes the physical walker had to be created. To do this a three dimensional model of the physical walker had to be constructed using Solid Works. The three dimensional Solid Works model is

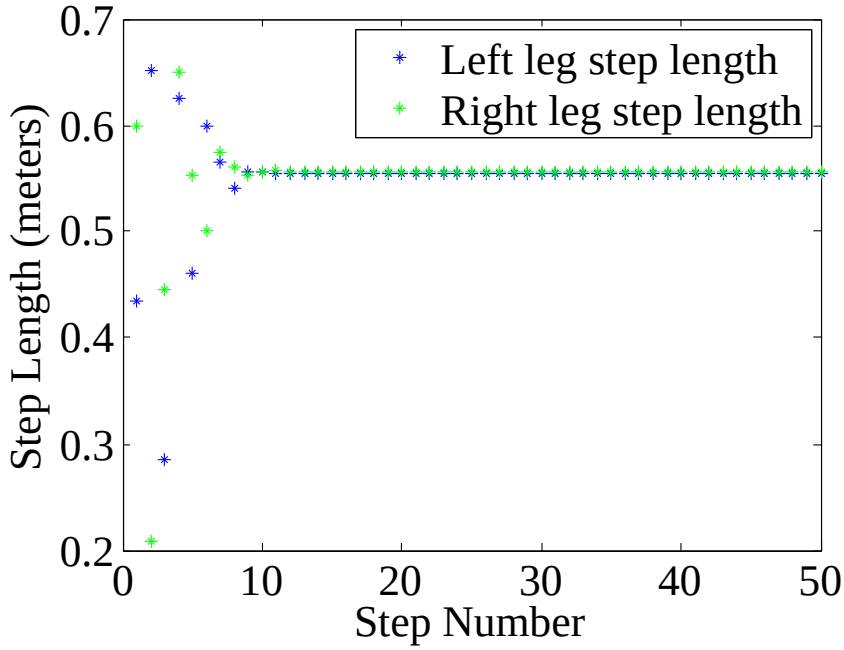

(a) Step length plot for the prosthesis model when the total mass is heavier and the gait patten is symmetric.

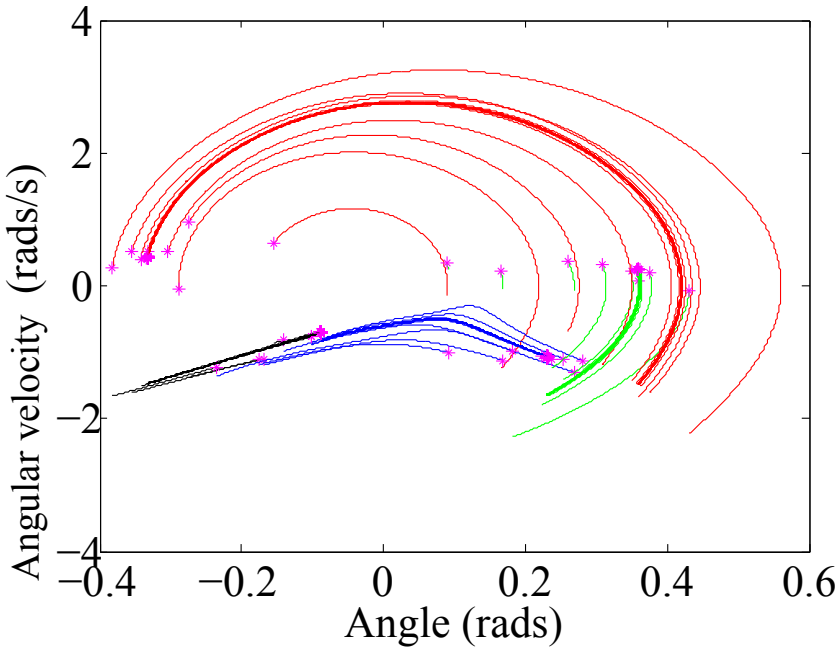

(b) Limit cycle plot for the prosthesis model when the total mass is heavier and the gait patten is symmetric.

Figure 4.10: The prosthesis symmetric gait pattern when the mass is heavier than the intact leg. This occurs when the prosthetic knee is in same location as the intact knee.

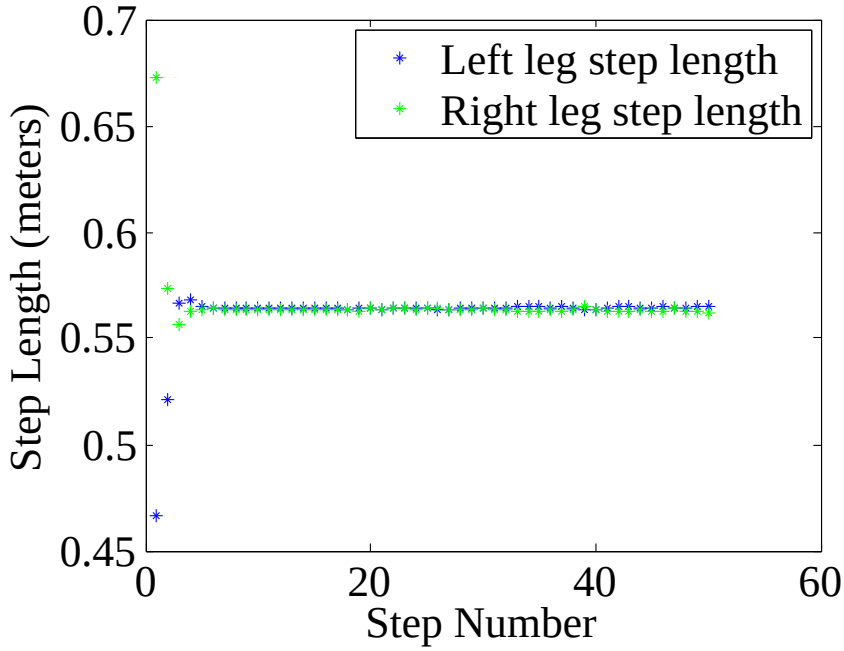

(a) Step length plot for the prosthesis model when the total mass is lighter and the gait patten is symmetric.

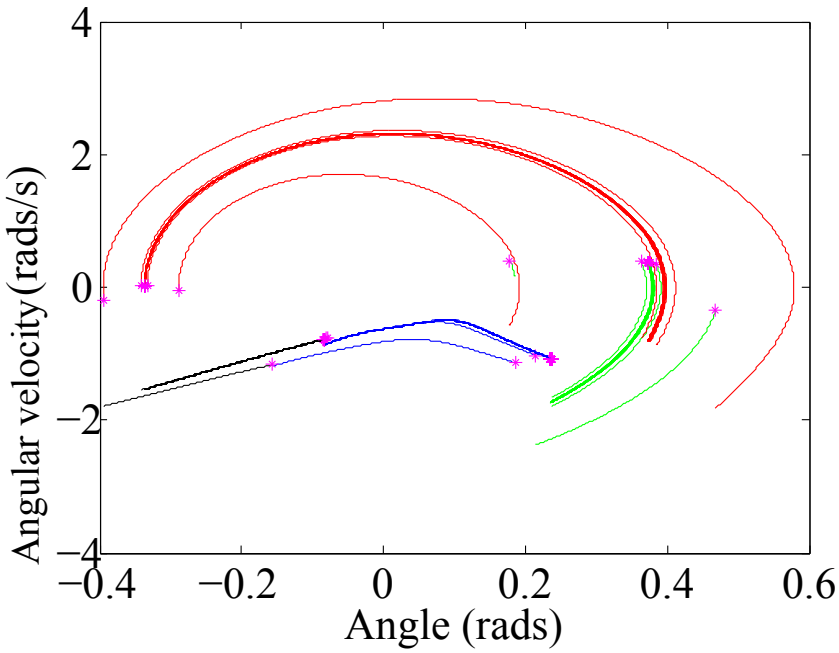

(b) Limit cycle plot for the prosthesis model when the total mass is lighter and the gait patten is symmetric.

Figure 4.11: The prosthesis symmetric gait pattern when the mass is lighter than the intact leg. This occurs when the prosthetic knee is moved down from the intact knee location by 36.7%. By doing this I have shown that moving the knee location can produce a symmetric gait with a lighter prosthesis

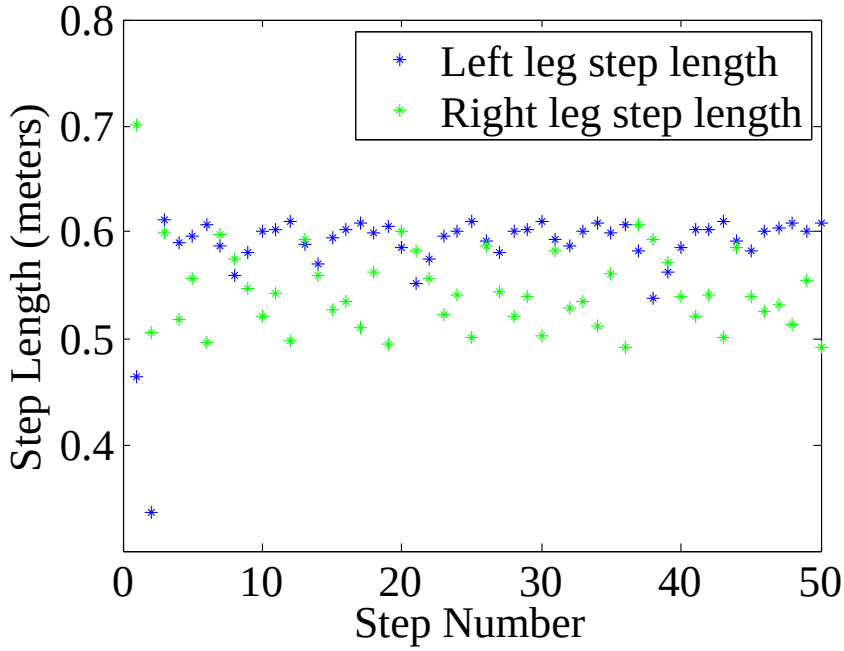

(a) Step length plot for the prosthesis model when the total mass is lighter and the gait patten is asymmetric.

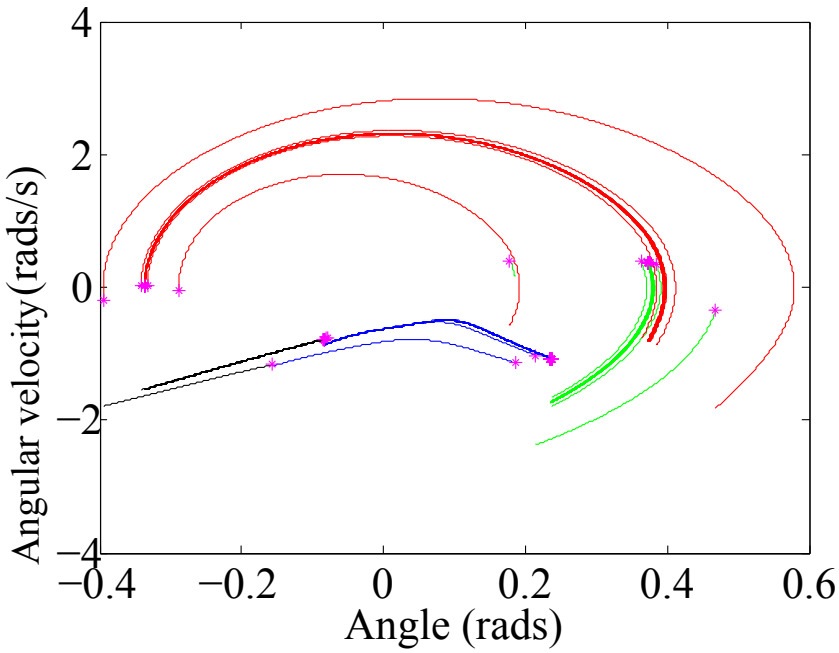

(b) Limit cycle plot for the prosthesis model when the total mass is lighter and the gait patten is asymmetric.

Figure 4.12: The prosthesis asymmetric gait pattern when the mass is lighter than the intact leg. This occurs when the prosthetic knee is moved down from the intact knee location by 42.8%. This goes past symmetry and creates an asymmetry that is opposite of a individual who wears a prosthetic.

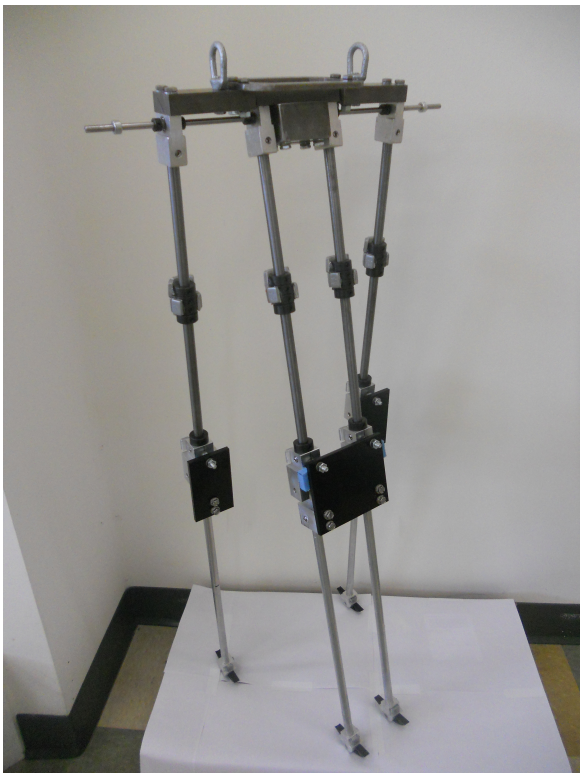

Figure 4.13: The picture of the physical walker. This is taken from [10]

seen in Figure 4.14. In the Solid Works model, different parts of the leg were coupled to create four large parts. The center of mass of these large parts were found using the Solid Works Mass Properties tool. These four center of masses represent the specific masses in the nine mass model. To check to make sure the masses and their locations were correct, the moment of inertia was calculated for the legs of the physical walker, the Solid Works model, and the physical walker model [10]. The moment of inertias of the three models were all within tolerances to prove that the locations in the theoretical model were correct.

The physical walker model did not have a steady and stable gait pattern when it was initially created. To correct for this unstable gait, different parameters were changed by a brute force search method until a stable gait was found. The results from this testing showed that the thigh and hip mass needed to be increased to produce a more stable gait. So weights were added to the physical PDW and the Solid Works model. Once again,

Figure 4.14: The Solid Works drawing the physical walker. This is taken from [10]

the centers of masses were found and checked in the physical walker model to make sure symmetry and stability were achieved [10].

The design and testing of the physical PDW is discussed in great detail in [10]. The author discusses the tuning of a physical passive dynamic walker and how it is a tedious and arduous task. This requires patience and a deep understanding of how the variables influence the stability of a physical PDW.

Chapter 5: Conclusions and Future Work

5.1 Conclusions

This research is an expansion of previous mathematical models that describe a passive dynamic walker (PDW). The current nine mass model allows for more adjustability, versatility, and better approximates the mass distribution of human legs. I have shown that the nine mass model is an improvement over its predecessor, the five mass model, which forces the center of mass to change with the moment of inertia. However, the nine mass model allows the center of mass and the moment of inertia to be changed independently of one another. Being able to adjust the mass locations for any specific walker combination allowed me to diminish the asymmetry that arises from having one leg longer than the other, derive the anthropomorphic model, create a theoretical prosthesis, and aid in the tuning of a physical PDW.

When an individual has one leg that is longer than the other, a large asymmetry arises. I found that adding a mass to the opposite leg's shank and thigh at a certain location would reduce the asymmetry. This is because the added masses are altering the dynamics of the normal leg enough to diminish the large asymmetry produced by the longer leg.

The anthropomorphic model describes the location and magnitude of the center of mass for each part of the human leg. This will better express the mass distribution of human legs and will aid in the testing of rehabilitation methods. The values for the locations and magnitudes of the center of masses were varied slightly to achieve a steady and stable

gait. The anthropomorphic model is important for modeling the theoretical transfemoral prosthesis that I described earlier. This prosthetic model breaks the assumption that the prosthetic knee needs to be in the same location as the intact knee. I was able to obtain a 68% decrease in the prosthetic shank and a 13.4% decrease in the total prosthetic mass while maintaining a symmetric gait pattern. This is accomplished by moving the location of the prosthetic knee below the location of the intact knee.

The nine mass model is also used to design and tune physical PDWs. Because of its large amount of adjustability of the model, it is easy to test a new design configuration before it is implemented on the physical PDW. This reduces the time spent in the tuning phase of physical PDW development.

This thesis showed the derivation of the nine mass model and some of the applications that it could be used for. The nine mass model is an improvement over the five mass model and has shown merit for rehabilitation because of the applications discussed in this thesis. The nine mass model will be further used for gait rehabilitation research, the design of rehabilitation devices and methods, and the design of physical PDWs.

5.2 Future Work

It has been shown that the nine mass model can be used for the application of gait rehabilitation design and testing. I have shown what rehabilitation methods I have tested and in this section, I will propose some other rehabilitation research that the nine mass model could be applied to in the future. The nine mass model could be extended to analyze how the joint torques affect the stress on the joints. This model could also be used to examine how spasticity, the tightness in the muscles arising from a stroke [19], affects gait patterns. Also, it would be important to validate the changing gait dynamics of the walker against a human participant.

5.2.1 Joint Torques

Prosthesis wearers tend to have joint pain and large amounts of stress at the prosthetic socket [22]. One cause of this discomfort is the asymmetry that is created from the prosthetic limb. The nine mass model could be adapted to analyze the forces and torques during walking. This could be done by summing the moments at the foot or the hip. There are two forces on the system, the force due to gravity (weight of the model) and the angular acceleration the model has during the dynamics. Similar to the optimization demonstrated in this thesis to reduce the asymmetry, the forces due to the angular acceleration could be optimized to reduce the torque on the joints and the stress at the prosthetic socket.

5.2.2 Spasticity

Spasticity is described as velocity dependent resistance to stretch or unusual tightness in muscles. This sometimes occurs in individuals who have suffered strokes [19]. This tightness could be implemented in the nine mass model to test rehabilitation methods to alleviate the asymmetry that arises from spasticity. To mimic the muscle tightness of spasticity, a velocity dependent damper and position dependent rotational spring could be applied to one of the knees and/or the hip. The following equation would describe this:

$$(J_i + J_a)\ddot{q} + (b_i + b_s)\dot{q} + (k_i + k_s)q = 0 \tag{5.1}$$

where J_i is the inherent moment of inertia at the specific joint, J_a is the added moment of inertia that arises from adding or changing masses. The damping parameters b_i and b_s are the rotational damping constants for the inherent damping in the joint and the added rotational damping for spasticity. The stiffness parameters k_i and k_s are the rotational

spring stiffness inherent in the joint and the added stiffness for spasticity. In the current work being done, $b_i = k_i = 0$. The inherent terms are need to model the inertia, damping, and stiffness present in the physical leg that is being simulated. The angular acceleration, velocity, and position are described by $\ddot{q}$, $\dot{q}$, and q respectively.

Similar to other tests presented in this paper the asymmetry that arises from the spring and the damper would be reduced by changing other parameters in this model.

5.2.3 Human Validation

Another important aspect for the nine mass model is comparing the motion of human walking to the dynamics described by the model. Some research has showed that increasing the mass and height of the foot on a participant will force the individual to curve toward the modified foot [10]. This means that the leg with the modified foot has a shorter step length. This agrees with the research done on the five mass passive dynamic walker model described in [11]. Further comparisons need to be made, for example comparing the prosthetic model to an individual who wears a prosthesis.

List of References

[1] Vanessa F. Hsu Chen. Passive Dynamic Walking with Knees: A Point Foot Model. Master's thesis, Massachusetts Institute of Technology, 2005.

[2] Julia T Choi, Eileen P G Vining, Darcy S Reisman, and Amy J Bastian. Walking flexibility after hemispherectomy: split-belt treadmill adaptation and feedback control. *Brain*, 132(Pt 3):722–733, Mar 2009.

[3] Steven H. Collins, Martijn Wisse, and Andy Ruina. A three-dimensional passive-dynamic walking robot with two legs and knees. *The International Journal of Robotics Research*, 20(7):607–615, 2001.

[4] Allison de Groot, Ryan Decker, and Kyle B. Reed. Gait enhancing mobile shoe (GEMS) for rehabilitation. In *Proc. Joint Eurohaptics Conf. and Symp. on Haptic Interfaces for Virtual Environment and Teleoperator Systems*, pages 190–195, March 2009.

[5] R. Drillis, R. Contini, M. Bluestein, Education United States. Dept. of Health, and Welfare. Vocational Rehabilitation Administration. *Body segment parameters: a survey of measurement techniques*. National Academy of Sciences, 1964.

[6] M. Garcia, A. Chatterjee, A. Ruina, and M. Coleman. The simplest walking model: Stability, complexity, and scaling. *Journal of Biomechanical Engineering*, 120(2):281–288, 1998.

[7] Ambarish Goswami, Benoit Thuilot, and Bernard Espiau. A Study of the Passive Gait of a Compass-Like Biped Robot. *The International Journal of Robotics Research*, 17(12):1282–1301, 1998.

[8] Robert D. Gregg, Amir Degani, Yasin Dhahe, and Kevin M. Lynch. The basic mechanics of bipedal walking lead to asymmetric behavior. In *Proc. IEEE Int. Conf. Rehabilitation Robotics*, pages 816–821, 2011.

[9] Ismet Handzic and Kyle B. Reed. Motion controlled gait enhancing mobile shoe for rehabilitation. In *Proc. IEEE Int. Conf. Rehabilitation Robotics*, 2011.

[10] Craig Honeycutt. Utilizing a computative model for the design of a passive dynamic walker. Master's thesis, University of South Florida, 2011.

[11] Craig Honeycutt, John Sushko, and Kyle B. Reed. Asymmetric passive dynamic walker. In *Proc. IEEE Int. Conf. Rehabilitation Robotics*, 2011.

[12] J.G.Daniel Karssen. Design and construction of the cornell ranger. Technical report.

[13] Rodolfo Margaria. *Biomechanics and energetics of muscular exercise*. Clarendon Press, 1976.

[14] Sarah J. Mattes, Philip E. Martin, and Todd D. Royer. Walking symmetry and energy cost in persons with unilateral transtibial amputations: Matching prosthetic and intact limb inertial properties. *Archives of Physical Medicine and Rehabilitation*, 81(5):561 – 568, 2000.

[15] Tad McGeer. Passive Dynamic Walking. *The International Journal of Robotics Research*, 9(2):62–82, 1990.

[16] Yuji Otoda, Hiroshi Kimura, and Kunikatsu Takase. Construction of a gait adaptation model in human split-belt treadmill walking using a two-dimensional biped robot. *Advanced Robotics*, 23:535–561, 2009.

[17] D. Reisman, H. Block, and A. Bastian. Interlimb Coordination During Locomotion: What Can be Adapted and Stored? *J. Neurophysiol*, 94(4):2403–2415, 2005.

[18] D. Reisman, R. Wityk, K. Silver, and A. Bastian. Locomotor adaptation on a split-belt treadmill can improve walking symmetry post-stroke. *Brain*, 130(7):1861–1872, 2007.

[19] Terence D. Sanger, Mauricio R. Delgado, Deborah Gaebler-Spira, Mark Hallett, and Jonathan W. Mink. Classification and definition of disorders causing hypertonia in childhood. *Pediatrics*, 111(1):e89–97, 2003.

[20] V.L. Talis, A.A. Grishin, I.A. Solopova, T.L. Oskanyan, V.E. Belenky, and Y.P. Ivanenko. Asymmetric leg loading during sit-to-stand, walking and quiet standing in patients after unilateral total hip replacement surgery. *Clinical Biomechanics*, 23(4):424 – 433, 2008.

[21] M. Wisse and J. Van Frankenhuyzen. Design and construction of mike; a 2d autonomous biped based on passive dynamic walking. In *Proceedings of International Symposium of Adaptive Motion and Animals and Machines (AMAM03*, 2003.

[22] M. Zhang, M. Lord, A.R. Turner-Smith, and V.C. Roberts. Development of a non-linear finite element modeling of the below-knee prosthetic socket interface. *Medical Engineering and Physics*, 17(8):559 – 566, 1995.

Appendices

Appendix A: Five Mass Model Derivation

For reference I have derived the five mass model dynamics. A portion of the derivation is also discussed in [11]. Similar to the nine mass model, the five mass model has two distinct phases in its dynamics: the two-link phase and the three-link phase. The five mass model's dynamics are derived using the Lagrangian formulation for a muti-pendulum system (A.1).

$$H(q)\ddot{q} + B(q,\dot{q})\dot{q} + G(q) = 0 \tag{A.1}$$

The three matrices in this equation H, B, and G are the inertia, velocity, and gravity matrices respectively.

A.1 Three-Link Dynamics

The three-link dynamics are described in the following equations by deriving the three Lagrangian matrices for a three-link pendulum system, similar to how it was done for the symmetric PDW in [1]. The matrices are as follows:

$$\begin{aligned} H11 &= ms_{st}a1_{st}^2 + mt_{st}(ls_{st} + a2_{st})^2 + \\ &\quad (mh + ms_{sw} + m_{sw})L_{st}^2 \end{aligned} \tag{A.2}$$

$$H12 = -(mt_{sw}b2_{sw} + ms_{sw}lt_{sw})L_{st}\cos(q_2 - q_1) \tag{A.3}$$

$$H13 = -ms_{sw}b1_{sw}L_{st}\cos(q_3 - q_1) \tag{A.4}$$

$$H21 = H12 \tag{A.5}$$

Appendix A: (continued)

$$H22 = mt_{sw}b2_{sw}^2 + ms_{sw}lt_{sw}^2 \tag{A.6}$$

$$H23 = ms_{sw}lt_{sw}b1_{sw}\cos(q_3 - q_2) \tag{A.7}$$

$$H31 = H13 \tag{A.8}$$

$$H32 = H23 \tag{A.9}$$

$$H33 = ms_{sw}b1_{sw}^2 \tag{A.10}$$

$$H = \begin{bmatrix} H11 & H12 & H13 \\ H21 & H22 & H23 \\ H31 & H32 & H33 \end{bmatrix} \tag{A.11}$$

$$h122 = -(mt_{sw}b2_{sw} + ms_{sw}lt_{sw})L_{st}\sin(q_2 - q_1) \tag{A.12}$$

$$h133 = -ms_{sw}b1_{sw}L_{st}\sin(q_3 - q_1) \tag{A.13}$$

$$h211 = -h122 \tag{A.14}$$

$$h233 = ms_{sw}lt_{sw}b1_{sw}\sin(q_3 - q_2) \tag{A.15}$$

$$h311 = -h133 \tag{A.16}$$

$$h322 = -h233 \tag{A.17}$$

$$B = \begin{bmatrix} 0 & h122\dot{q}_2 & h133\dot{q}_3 \\ h211\dot{q}_2 & 0 & h233\dot{q}_3 \\ h311\dot{q}_1 & h322\dot{q}_2 & 0 \end{bmatrix} \tag{A.18}$$

$$\begin{aligned} g_1 &= -(ms_{st}a1_{st} + mt_{st}(ls_{st} + a2_{st}) + \\ &\quad (mh + ms_{sw} + mt_{sw})L_{sw})\sin(q_1)g \end{aligned} \tag{A.19}$$

Appendix A: (continued)

$$g_2 = (mt_{sw}b2_{sw} + ms_{sw}lt_{sw})\sin(q_2)g \tag{A.20}$$

$$g_3 = ms_{sw}b1_{sw}\sin(q_3)g \tag{A.21}$$

$$G = [g_1 \;\; g_2 \;\; g_3]^T \tag{A.22}$$

A.2 Two-Link Dynamics

The two-link dynamics are described by the Lagrangian of a double pendulum system. The matrices are as follows:

$$\begin{aligned} H11 &= ms_{st}a1_{st}^2 + mt_{st}(ls_{st} + a2_{st})^2 + \\ &\quad (mh + ms_{sw} + mt_{sw})L_t^2 \end{aligned} \tag{A.23}$$

$$\begin{aligned} H12 &= -(mt_{sw}b2_{sw} + ms_{sw}(lt_{sw} + \\ &\quad b1_{sw}))L_{st}\cos(q_2 - q_1) \end{aligned} \tag{A.24}$$

$$H21 = H12 \tag{A.25}$$

$$H22 = mt_{sw}b2_{sw}^2 + ms_{sw}(lt_{sw} + b1_{sw})^2 \tag{A.26}$$

$$H = \begin{bmatrix} H11 & H12 \\ H21 & H22 \end{bmatrix} \tag{A.27}$$

$$h = -(mt_{sw}b2_{sw} + ms_{sw}(lt_{sw} + b1_{sw}))L_{st}\sin(q_2 - q_1) \tag{A.28}$$

$$B = \begin{bmatrix} 0 & h\dot{q}_2 \\ -h\dot{q}_1 & 0 \end{bmatrix} \tag{A.29}$$

Appendix A: (continued)

$$\begin{aligned} g_1 &= -(ms_{st}a1_{st} + mt_{st}(ls_{st} + a2_{st}) + \\ &\quad (mh + ms_{sw} + mt_{sw})L_{sw})\sin(q_1)g \end{aligned} \tag{A.30}$$

$$g_2 = (mt_{sw}b2_{sw} + ms_{sw}(lt_{sw} + b1_{sw}))\sin(q_2)g \tag{A.31}$$

$$G = [g_1 \;\; g_2]^T \tag{A.32}$$

A.3 Collision Events

In [11] only the dynamics were derived the collisions were omitted due to space limitations. I am showing the derivation of the five mass model collisions for reference.

The following equations take the pre-collision velocities (q^-) and apply conservation of angular momentum and output the post-collision velocities (q^+). It is to be noted that the superscript $+$ is post-collision and $-$ is pre-collision.

A.3.1 Knee Strike

$$\begin{bmatrix} \dot{q_1}^+ \\ \dot{q_2}^+ \end{bmatrix} = Q^{+^{-1}} \begin{bmatrix} \dot{q_1}^- \\ \dot{q_2}^- \\ \dot{q_3}^- \end{bmatrix} Q^- \tag{A.33}$$

$$\alpha = q_1 - q_2 \tag{A.34}$$

$$\beta = q_1 - q_3 \tag{A.35}$$

$$\gamma = q_2 - q_3 \tag{A.36}$$

$$Q_{11}^+ = Q_{21}^+ + mt_{st}(ls_{st} + a2_{st})^2 + (mh + mt_{st} + ms_{st})L_{st}^2 + ms_{st}a1_{st}^2 \tag{A.37}$$

Appendix A: (continued)

$$Q_{11}^{+} = Q_{21}^{+} + ms_{sw}(lt_{sw} + b1_{sw})^2 + mt_{sw}b2_{sw}^2 \tag{A.38}$$

$$Q_{21}^{+} = -(ms_{sw}(b1_{sw} + ltsw) + mt_{sw}b2_{sw})\cos\alpha \tag{A.39}$$

$$\begin{aligned} Q_{11}^{-} = &-(ms_{sw}lt_{sw} + mt_{sw}b2_{sw})L_{st}\cos(\alpha) - ms_{sw}b1_{sw}L_{st}\cos(\alpha) + \\ &(mt_{sw} + ms_{sw} + mh)L_{st}^2 + ms_{st}a1_{st}^2 + mt_{st}(ls_{st} + a2_{st})^2 \end{aligned} \tag{A.40}$$

$$\begin{aligned} Q_{12}^{-} = &-(ms_{sw}lt_{sw} + mt_{sw}b2_{sw})L_{st}\cos(\alpha) + ms_{sw}b1_{sw}lt_{st}\cos(\gamma) + \\ &mt_{sw}b2_{sw}^2 + ms_{st}lt_{sw}^2 \end{aligned} \tag{A.41}$$

$$Q_{13}^{-} = -ms_{sw}b1_{sw}L_{st}\cos(\beta) + ms_{sw}b1_{sw}lt_{sw}\cos(\gamma) + ms_{sw}b1_{sw}^2 \tag{A.42}$$

$$Q_{21}^{-} = -(ms_{sw}lt_{sw} + mt_{sw}b2_{sw})L_{st}\cos(\alpha) - ms_{sw}b1_{sw}L_{st}\cos(\beta) \tag{A.43}$$

$$Q_{22}^{-} = ms_{sw}b1_{sw}lt_{sw}\cos(\gamma) + ms_{sw}lt_{sw}^2 + mt_{sw}b2_{sw}^2 \tag{A.44}$$

$$Q_{23}^{-} = ms_{sw}b1_{sw}lt_{sw}\cos(\gamma) + ms_{sw}b1_{sw}^2 \tag{A.45}$$

$$Q^{+} = \begin{bmatrix} Q_{11}^{+} & Q_{12}^{+} \\ Q_{12}^{+} & Q_{22}^{+} \end{bmatrix} \tag{A.46}$$

$$Q^{-} = \begin{bmatrix} Q_{11}^{-} & Q_{12}^{-} & Q_{13}^{-} \\ Q_{12}^{-} & Q_{22}^{-} & Q_{23}^{-} \end{bmatrix} \tag{A.47}$$

A.3.2 Heel Strike

$$q^{+} = \begin{bmatrix} q_2^{-} \\ q_1^{-} \\ q_1^{-} \end{bmatrix} \tag{A.48}$$

Appendix A: (continued)

$$\begin{bmatrix} \dot{q_1}^+ \\ \dot{q_2}^+ \\ \dot{q_3}^+ \end{bmatrix} = Q^{+^{-1}} \begin{bmatrix} \dot{q_1}^- \\ \dot{q_2}^- \end{bmatrix} Q^- \tag{A.49}$$

$$\dot{q}_3^+ = \dot{q}_2^+ \tag{A.50}$$

$$\alpha = q_1 - q_2 \tag{A.51}$$

$$\begin{aligned} Q_{11}^+ = Q_{21}^+ + (ms_{sw} + mt_{sw} + mh)L_{sw}^2 + ms_{sw}a1_{sw}^2 + \\ mt_{sw}(a2_{sw} + ls_{sw})^2 \end{aligned} \tag{A.52}$$

$$Q_{12}^+ = Q_{21}^+ + ms_{st}(b1_{sw} + lt_{sw}) + mt_{sw}b2_{sw}^2 \tag{A.53}$$

$$Q_{21}^+ = -(ms_{st}(b1st + lt_{st}) + mt_{st}b2_{sw})L_{sw}\cos(\alpha) \tag{A.54}$$

$$Q_{22}^+ = ms_{sw}(lt_{sw} + b1_{sw})^2 + mt_{sw}b2_{sw}^2 \tag{A.55}$$

$$Q_{11}^- = Q_{12}^- + (mhL_{st} + 2mt_{st}(a2_{st} + ls_{st}) + ms_{st}a1_{st})L_{st}\cos(\alpha) \tag{A.56}$$

$$Q_{12}^- = -(ms_{sw}a1_{sw}(lt_{sw} + b1_{sw}) + mt_{sw}b2_{sw}(ls_{sw} + a2_{sw})) \tag{A.57}$$

$$Q_{21}^- = Q_{12}^- \tag{A.58}$$

$$Q_{22}^- = 0 \tag{A.59}$$

$$Q^+ = \begin{bmatrix} Q_{11}^+ & Q_{12}^+ \\ Q_{12}^+ & Q_{22}^+ \end{bmatrix} \tag{A.60}$$

$$Q^- = \begin{bmatrix} Q_{11}^- & Q_{12}^- \\ Q_{12}^- & Q_{22}^- \end{bmatrix} \tag{A.61}$$